Arabian Journal of Geosciences (2022) 15: 1070
https://doi.org/10.1007/s12517-022-09764-2

ORIGINAL PAPER

Organic geochemical and petrological evaluation to assess the remaining hydrocarbon potential and depositional conditions: a case study of the Paleozoic shales of west Perlis region, northern Peninsular Malaysia

Muhammad Nadzmi Abdul Ghofur[1] · Jasmi Hafiz Abdul Aziz[1] · Yousif M. Makeen[2] · Wan Hasiah Abdullah[3] · Mohammed Hail Hakimi[4]

Received: 22 January 2021 / Accepted: 23 February 2022 / Published online: 27 May 2022

Abstract

The shale samples of the Timah Tasoh Formation that deposited during the Early Devonian in Perlis, northern Peninsular Malaysia, have been investigated by utilising organic geochemical and petrological methods as well as elemental compositions. The shale samples were examined to assess the origin, type, and conditions of the paleodepositional environment during the sediment deposition and explore the gas-generating potential from the conversion of bitumen to gas from the more profound and older Paleozoic strata. Biomarker study indicates a mixed terrestrial-derived organic matter input with significant influences from lacustrine and marine-derived (marine phytoplanktonic-bacteria) land-plants organic matter deposited in a transitional environment (terrestrial to marine) under a suboxic condition. The ratio of trace elements concentration (e.g. Sr, Ba, V, Ni, Cr) established that the organic material was preserved under suboxic to oxic conditions. The analysis from the Rock–Eval pyrolysis indicates poor to very good hydrocarbon source potentials. However, evaluation based on bulk pyrolysis shows that the Timah Tasoh Formation contains a low hydrogen index (HI), suggesting that the organic matter is dominated by type IV kerogen, corroborated by the high vitrinite reflectance values. It indicates that the analysed samples are already in the stage of late mature to overmature and thus within a gas generation window. The solid bitumen within samples suggests that the Timah Tasoh Formation had prominent organic matter content for liquid hydrocarbon generation before a thick overburden rock and high thermal temperature occurred at the beginning of the deposition. During Late Cretaceous time transformed the primary organic matter kerogens of types II and III (that initially generated liquid hydrocarbons) into type IV kerogen, generating thermogenic gas potential by the process of secondary cracking source rocks.

Keywords Hydrocarbon source potential · Thermal maturity · Kerogen types · Biomarker fingerprints · Solid bitumen · Thermogenic gas · Perlis Timah Tasoh shales

Responsible Editor: Santanu Banerjee

✉ Jasmi Hafiz Abdul Aziz
jasmihafiz@um.edu.my

✉ Yousif M. Makeen
makeen.geo@hotmail.com

[1] Department of Geology, University of Malaya, 50603 Kuala Lumpur, Malaysia

[2] College of Earth Science, Jilin University, Changchun 130061, China

[3] Geological Society of Malaysia, c/o Department of Geology, University of Malaya, 50603 Kuala Lumpur, Malaysia

[4] Geological Department, Faculty of Applied Science, Taiz University, 6803 Taiz, Yemen

Introduction

The shale within the Timah Tasoh Formation has caught the attention of various studies of interest, particularly in sedimentary and sequence stratigraphy aspects (e.g. Foo 1983; Hassan and Lee 2005; Hassan et al. 2014; Baioumy et al. 2016). However, detailed research on the hydrocarbon source rock potential from this older sequence is still lacking. Numerous studies on this type of older and deeper sequence shales have shown a significant hydrocarbon potential and will most likely serve as unconventional and gaseous hydrocarbons (e.g. Hunt 1996; Zou et al. 2019). As examples, a lot of researchers around the world have recently

been fascinated by the importance of unconventional hydrocarbons studies, especially in shale gas potential (e.g. Dardour et al. 2004; Soua 2014; Gasparrini et al. 2014; Tunstall 2015; Vanhazebroeck & Borrok 2016; Hakimi et al. 2020). The rapid development of unconventional hydrocarbons in the USA, especially shale gas from the sediment deposits of the Paleozoic Era, such as the Marcellus Formation, the Barnett Shale, the Woodford Shale and the Eagle Ford Formation, has shown that this resource can be commercialised (Scrotchman 2016). Therefore, the Paleozoic Era formation sequence quickly became the main hydrocarbon target areas (Soua 2014).

Nowadays, shale gas is becoming a vital hydrocarbon production goal, resulting in increased scientific research on mudrock or organic-rich shales, generating hydrocarbons (gas/oil) either through biogenic or thermogenic approaches (Tourtelot Harry 1979; Jarvie et al. 2007; Newport Leo et al. 2016). The shale gas could be produced from the sedimentary formations that show characteristics such as older stratigraphic layer, deep burial formations, and high thermal maturity area and had exposure to various tectonic activities (Dai et al. 2014; Zou et al. 2015). For instance, Zumberge et al. (2012) identified the geochemistry of the effective shale gas formations of North America, such as the Devonian Woodford Formation in the Arkoma Basin, with have > 2.0 wt% TOC, type I, II kerogen, and high thermal maturity from vitrinite reflectance values (1.1 to 3.0%Ro). Similarly, some countries, such as China, display a high TOC value (1.6 to 6.8 wt%) of shale source rock from the Silurian Longmaxi Formation of the Zhaotong block. That produced types I and II kerogens and high thermal maturity (2.1 to 3.0%Ro) produced from the burial of older deeper sediments (Zou et al. 2014).

The relationship between bitumen-to-thermogenic gas potential from the high thermal maturity source rock environments has now been widely studied around the world (e.g. Etiope et al. 2013; Pytlak et al. 2016; Xiong et al. 2016; Hakimi et al. 2020; Maeyama et al. 2020). Jarvie et al. (2007) and Zou et al. (2015) have classified the sources of thermogenic shale gas in the hydrocarbon basin into three categories which are kerogeneous (insoluble organic matter), bitumen (soluble organic matter) and pyrobitumen (cracking bitumen residue). Sources in which secondary bitumen cracking process of source rock can generate unconventional gases (Rooney et al. 1995). Therefore, the bitumen-to-gas production is highly dependent on the shale efficiency and efficacy for hydrocarbon expulsion, and the production of gas depends on its high levels of thermal maturity and geological environment (Rooney et al. 1995; Lewan and Henry 2001).

Palaeozoic age rocks are widely distributed in northern states of Malaysia, (e.g. Perlis, Fig. 1). This northern area is assumed to have a deposition of older shaly sediments that could act as an essential unconventional hydrocarbon resource (Baioumy et al. 2016). The geological characteristics of this area in terms of tectonic evolution, stratigraphy, and sedimentology have been studied by numerous researchers (Burton 1970; Jones 1981; Foo 1983; Lee 2001; Hassan & Lee 2005; Cocks et al. 2005; Azman 2009; Metcalfe 2013b; Hassan et al. 2014). However, shale gas studies especially thermogenic gas potential studies are still lacking in Malaysia and also Southeast Asia. Therefore, further analysis into the source and development process of these highly mature/overmature shale rocks is considered essential for shale gas exploration in Malaysia (Nugraheni et al. 2013), especially in terms of the potential of thermogenic gas resources.

Therefore, in this study, an evaluation of the hydrocarbon generation potential of the Paleozoic shales from the central Perlis area in Malaysia was conducted. The main objectives of this study are (a) to understand the depositional condition setting of the source rock and (b) to determine the source rock potential for hydrocarbon generation. This study applies a combination of organic, inorganic geochemical methods and organic petrological analysis that incorporates biomarker fingerprints and elemental composition analysis to interpret the depositional environments and also to assess the remaining hydrocarbon source potential including the thermogenic gas potential in the study area. This would provide information on the shale gas potential generated by deep-oil source rocks that could be associated with many other potential thermogenic gas basins globally, thereby enabling future exploration of the new petroleum resource region.

Geological setting

During the Paleozoic Era, there were significant tectonic changes that occur on the Earth; thus, it is of great interest to geoscientists. The Paleozoic Era witnessed the breakup of supercontinent Rodinia and the formation of supercontinent Pangaea. The Paleozoic Era also reflects an enormous outbreak of life on Earth that started during the Cambrian Explosion and resulted in the largest mass extinction in the world, known as the Permian–Triassic event of extinction, extinguishing up to 95% of the planet's life. In Peninsular Malaysia, the Paleozoic Era has seen various geological evolutions which resulted from the collision between the Sibumasu Terrane and the Sukhothai Arc along the Bentong-Raub suture zone that occurred in the early Triassic. The collision led to the development of three longitudinal north–south tectonostratigraphic belts which are Western, Central and Eastern belts with distinct variations in stratigraphy, composition, magmatism, volcanism, types of mineralisation, geophysical signatures and geological evolution

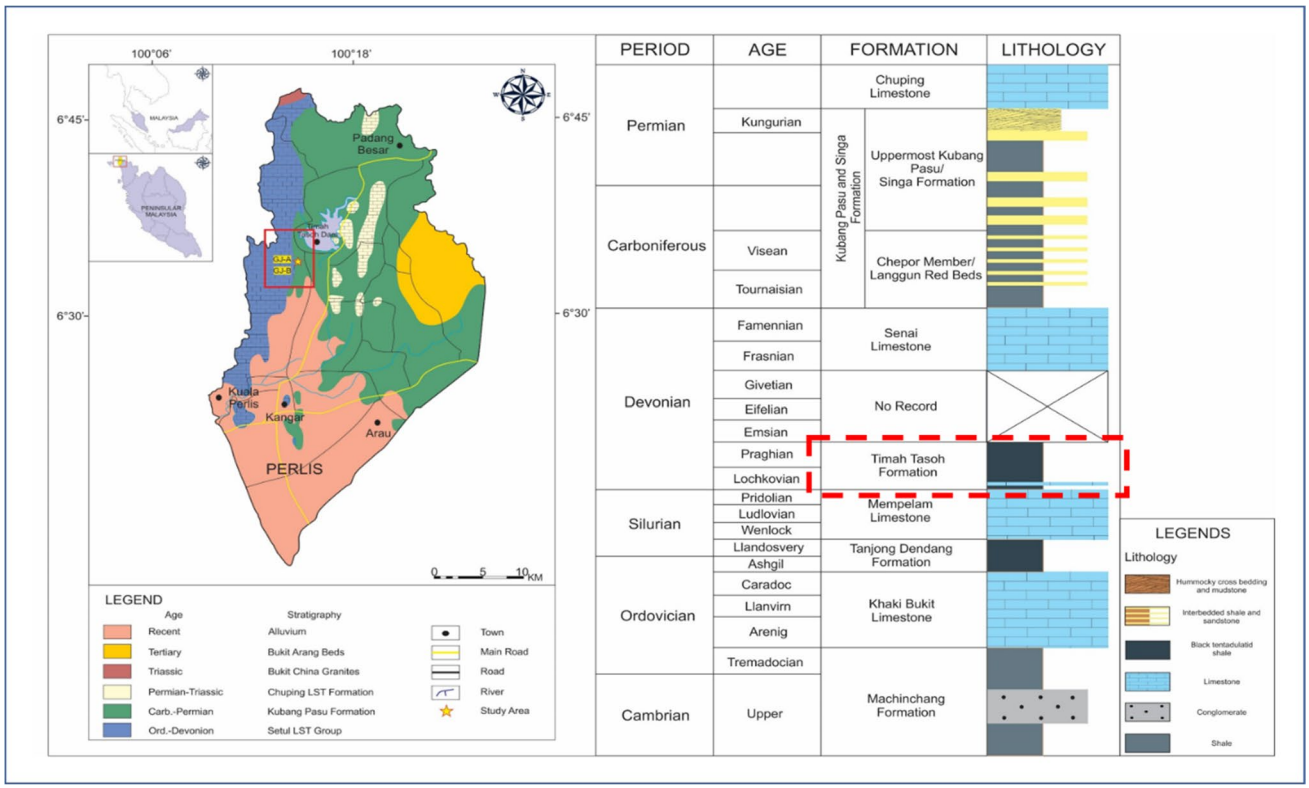

Fig. 1 The location of the study areas within central Perlis and simplified sedimentary logged section of the studied Paleozoic rock samples in the northern part of Peninsular Malaysia. The geological map and stratigraphy section shown is adapted after Hassan (2013).

(Scrivenor 1928; Khoo and Tan 1983; Metcalfe 2013a, 2017).

Around 25% of the Malay Peninsula is covered by Paleozoic rocks (Lee et al. 2004; Lee 2009), with Lower Palaeozoic rocks restricted to the Western Belt. However, the Upper Paleozoic rocks are distributed in all three tectonostratigraphic belts in Peninsular Malaysia. Metcalfe (1988) proposed that Peninsular Malaysia have consisted of two continental terranes, a Western Gondwana affinity continental Terrane (Sibumasu) and an Eastern Cathaysian affinity continental Terrane (Indochina/East Malaya). The Sibumasu Terrane is characterised by a Paleozoic passive margin sequence which includes a belt of Late Carboniferous to Early Permian glacial marine diamictite (Staufer & Mantajit 1981; Metcalfe 1988). These Early Permian faunas have a high-latitude, cold-water Gondwana affinity and thus correspond with the Western Belt of Peninsular Malaysia (Khoo & Tan 1983). In the north-western part of Peninsular Malaysia, where the study area is located, the complete Palaeozoic series on the peninsula, ranges in age from Upper Cambrian to Upper Permian, can be founded (Fig. 1) (Cocks et al. 2005; Hassan and Lee 2005; Lee et al. 2004; Lee 2009). Nevertheless, only shales containing formations, viz., the Early Devonian Timah Tasoh Formation, are being studied using organic geochemical methods to evaluate their hydrocarbon source potential and interpret their deposition conditions.

Tectonically, the sedimentary deposition of the area is situated at a far distance from a granitic intrusion and is therefore not significantly affected by metamorphic interaction. However, they were affected by regional metamorphism caused by the Western Belt of Peninsular Malaysia orogenic and subduction events (Ghani et al. 2013; Metcalfe 2013b). In addition, Madon (1993) and Tjia (1998) report that a significant deformation event has occurred during Late Cretaceous times as it was associated with a formation of a mantle spot located offshore of Peninsular Malaysia. The formation of mantle hot spot is due to the crustal extension in Malay Basin, which caused a circular regional uplift around 1000 km. Widespread from the hotspot location, which covered all parts of Peninsular Malaysia (Tjia 1998), gives a high heat flow to the surrounding area (Fig. 2).

Timah Tasoh Formation

The Timah Tasoh Formation, previously recognised as the "Upper Detrital Member" Setul Formation (Jones 1973, 1981), is an onshore sedimentary formation that formed during Paleozoic orogenic tectonic rifting events. This Devonian stratigraphic formation is characterised by graptolites and

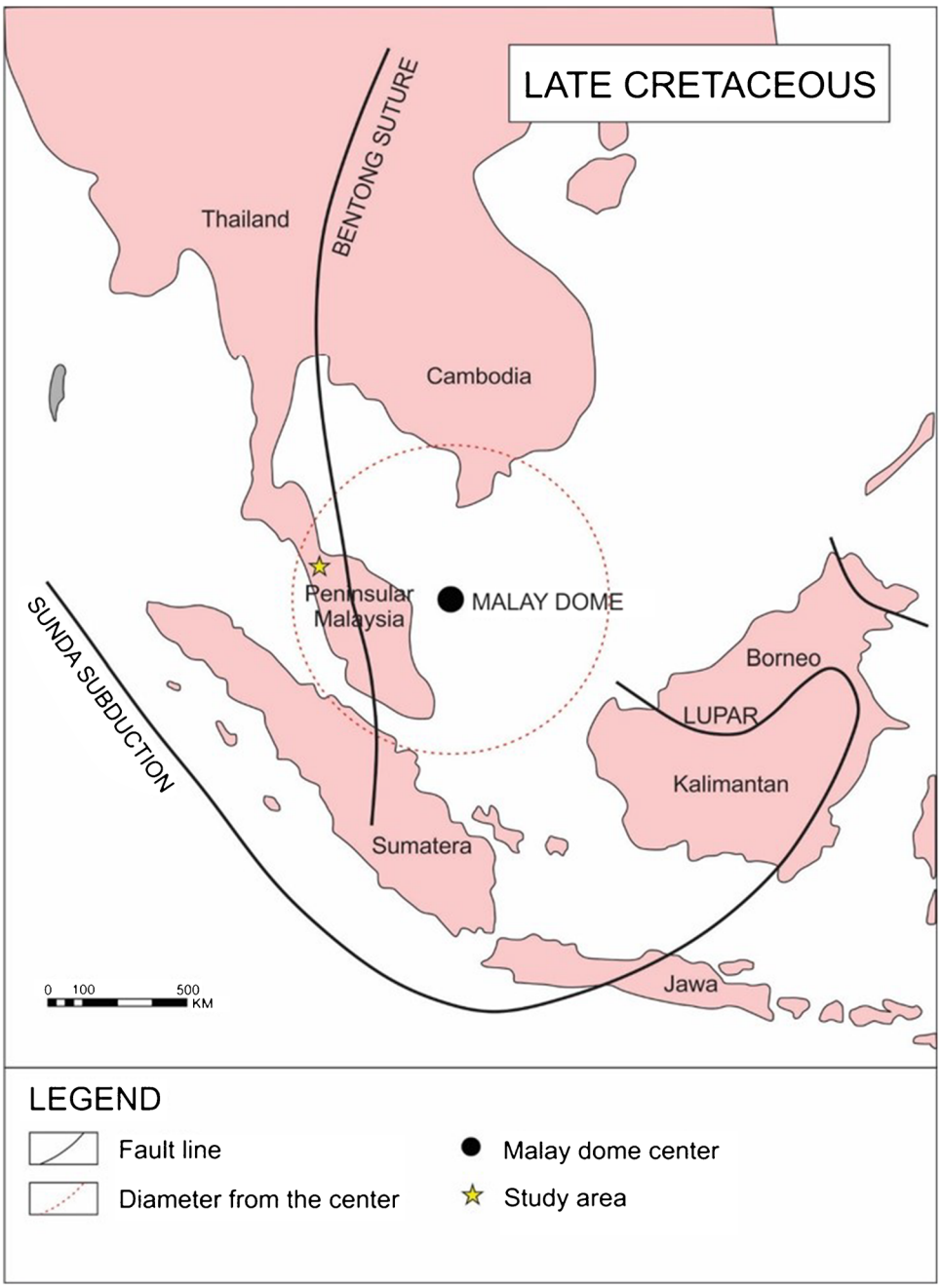

Fig. 2 The location of mantle plum or hotspot that created a Malay dome during Late Cretaceous

tentaculitids forming, with occasional cherts, black shales and mudstones. According to Hassan et al. (2013), the formation gives abundant tentaculitid dacryoconarides, including Styliolina sp., Metastyliolina? sp., M. Lardeuxi, Nowakia acuaria acuaria (Turkestanella), Nowakia (T.) acuaria posterior, and Nowakia (Alaina) matlockiensis. The graptolites Monograptus cf. uniformis and M. langgunensis and the brachiopod Plectodonta (P.) forteyi and the trilobite Plagiolaria are also found associated with the tentaculitids (Jones 1973; Hassan and Lee 2005; Hassan et al. 2014; Metcalfe 2017). The presence of tentaculitides and graptolites indicates that the formation during late Pragian (410 Ma) or earliest Emsian was deposited in an anoxic-dysoxic, marine outer shelf setting with a water depth of between 150 and 200 m (Brett and Baird 1993; Boucot et al. 1999; Hassan and Lee 2005; Hassan et al. 2014).

Samples and methods

Approximately 15 shale samples from the Timah Tasoh Formation outcrop were collected for this analysis. These samples were subsequently examined by applying organic

geochemical methods to characterise the type and origin of the organic matter, paleodepositional environment, and thermal maturity to assess their hydrocarbon generation potential. All the samples were collected through the fieldwork by considering non-weathered exposures and oxidised surface (about 20 cm deep) to avoid possible weathering effect commonly associated with outcrop samples. The sampling locations are recorded and shown in Fig. 1 with the location coordinates presented in Table 1.

Organic geochemical methods

The Rock–Eval/TOC analysis has been used as a screening method to identify and select samples for subsequent analysis such as vitrinite reflectance and biomarker analysis. The total organic carbon (TOC) values and Rock–Eval parameters are as provided in Table 1. During the preparation for Rock–Eval pyrolysis, the shales were pulverised into fine-grade powder and were examined using a Rock–Eval 6 machine fitted with a TOC module. Around 100 mg powder samples were heated and pyrolyzed from 100 to 850 °C to obtain the parameters needed in determining source rock potentials such as the TOC, S_1, S_2, S_3, and the temperature of maximum pyrolysis yield (T_{max}). The other parameters such as hydrogen index (HI), production index (PI) and production yield (PY) are as explained by previous researchers (e.g. Espitalie et al. 1977; Peters and Cassa 1994; McCarthy et al. 2011) were also presented (Table 2).

About 10 to 15 g of finely pulverised shale samples with TOC more than 0.5 wt% were used for the bitumen extraction analysis for 72 h of extraction by using the Soxhlet apparatus. Bitumen extraction was performed to acquire the extractable organic matter (EOM) or bitumen and hydrocarbon content of the analysed samples. A combination solution of dichloromethane (CH_2CI_2) and methanol (CH_3OH) with a ratio of 93:7 was used as the solvent to extract organic matter. The EOM was separated into specific components using a liquid column chromatography method. Increasing the polarity of the solvents such as petroleum ether, dichloromethane and methanol was applied to fractionate saturated hydrocarbon, aromatic hydrocarbon and NSO compounds for the biomarker analyses. An analysis using gas chromatography-mass spectrometry (GCMS) was executed using an Agilent 5975B inert MSD mass spectrometer instrument. The saturated and aromatic compounds were examined for biomarker fingerprint analysis. The GCMS analysis was conducted using an HP-5MS column heated with the temperature from 40 to 300 °C, rate of 4 °C/min and 30 min hold at temperature 300 °C. The mass spectrometer instrument was directly connected to the 70 eV ionisation voltage ion source, 100 mA filament emission current and 230 °C interface temperature.

Based on the GCMS, the *n*-alkanes and isoprenoids were analysed using a mass chromatogram of ion *m/z* 85, and terpanes and triterpanes were using *m/z* 191, while steranes and diasteranes were analysed using *m/z* 217 (Appendix Table 4). All of the components were examined and calculated by measuring the peak height and comparing the retention times with the relative abundances by referring to the procedure of calculation from the earliest researchers (e.g. Radke et al. 1986; Peters and Moldowan 1993; Makeen et al. 2015; Hakimi et al. 2016; Ayinla et al. 2017). The results of the analysed samples are presented in Table 2.

Inorganic geological methods

The amounts of major oxides and trace elements of the Timah Tasoh Formation were determined using a plasma mass spectrometer (ICP-MS) coupled with an Agilent inductive spectrometer following the GCMS analysis. To complete the digestion, a PerkinElmer Titan MPS microwave oven digested about 0.50 g of the samples using HNO_3, HF, and HCl, and finally H_3BO_3 was applied to complete the digestion process. The solution was eventually diluted with ultimate pure water up to 100. The research used a standard solution of elements with an analytic concentration of 10 ppm, and a minimum detection limit of less than 1 ppb was used for the instrument calibration. The results of the major oxides and trace elements are shown in Table 3.

Organic petrological methods

In addition to geochemical methods, petrographic studies were also conducted to determine the type of kerogen and the thermal maturity of the samples analysed. Polished blocks of the samples were made by mounting fine grades of crushed rock samples (about 3 mm in size) inside a slow setting polyester of Serrifix resin mixed along with resin hardener and were left to harden. After 3 days, the hardened blocks were grounded using a grinder machine. Subsequently, they polished the surfaces using silicon carbide sandpaper from decreasing coarse texture by applying isopropyl alcohol as an emollient polished using finer alumina powder with decreasing grades to produce smooth reflecting surfaces. The petrographic analysis was carried out by observing under a Leica microscope (DM6000M) and Leica photometry system (CTR6000) which were fitted with fluorescence illuminators under a white plane-polarised reflected light. Vitrinite reflectance measurements were conducted using a × 50 objective under immersion oil with 1.518 refractive indexes at 23 °C. The mean random (15 to 30 measurements) vitrinite reflectance was calculated and performed using the Diskus Fossil software in the Windows programme. The calculated values for reflectance are as shown in Table 1.

Table 1 Locations and lithology types of the analysed samples and results of geochemical and optical methods, including TOC content, Rock–Eval pyrolysis and vitrinite reflectance (%VR_O) measurements

Formation	Location	Sample ID	GPS coordinates	Lithology	TOC Wt.%	Rock–Eval pyrolysis data						(%VR_O)	(%SBRo)
						S_1(mg/g)	S_2(mg/g)	PY (mg/g)	T_{max} (°C)	HI (mg/g)	PI (mg/g)		
Timah Tasoh	GJ-A	GJ-A1-SH	N06° 33′ 7.20″, E100° 14′ 11.39 ″	Shale	0.64	0.02	0.00	0.02	602	0.00	1.00	1.93	-
		GJ-A2-SH	N06° 33′ 7.20″, E100° 14′ 11.39 ″	Shale	0.51	0.02	0.00	0.02	601	0.00	1.00	1.22	1.05
		GJ-A3-SH	N06° 33′ 7.20″, E100° 14′ 11.39 ″	Shale	1.27	0.04	0.02	0.06	600	1.57	0.67	1.43	1.29
		GJ-A4-SH	N06° 33′ 7.20″, E100° 14′ 11.39″	Shale	2.83	0.11	0.07	0.18	584	2.47	0.61	1.67	1.35
		GJ-A5-SH	N06° 33′ 7.20″, E100° 14′ 11.39″	Shale	0.54	0.03	0.00	0.03	582	0.00	1.00	1.20	1.06
		GJ-A6-SH	N06° 33′ 7.20″, E100° 14′ 11.39″	Shale	2.64	0.05	0.03	0.08	603	1.14	0.63	1.48	1.22
		GJ-A7-SH	N06° 33′ 7.20″, E100° 14′ 11.39″	Shale	5.28	0.39	0.17	0.56	603	3.22	0.70	1.52	1.39
		GJ-A8-SH	N06° 33′ 7.20″, E100° 14′ 11.39″	Shale	1.56	0.03	0.02	0.05	601	1.28	0.60	1.23	1.11
		GJ-A9-SH	N06° 33′ 7.20″, E100° 14′ 11.39″	Shale	1.09	0.04	0.02	0.07	600	1.83	0.67	1.32	1.20
		GJ-A10-SH	N06° 33′ 7.20″, E100° 14′ 11.39″	Shale	2.31	0.04	0.05	0.09	602	2.16	0.44	1.41	1.28
		GJ-A11-SH	N06° 33′ 7.20″, E100° 14′ 11.39″	Shale	2.00	0.03	0.03	0.06	601	1.50	0.50	1.25	1.12
		GJ-A12-SH	N06° 33′ 7.20″, E100° 14′ 11.39″	Shale	1.67	0.04	0.02	0.06	600	1.20	0.67	1.36	1.23
	GJ-B	GJ-B1-SH	N06° 32′ 56.08″, E100° 14′ 13.76″	Shale	0.39	0.03	0.00	0.03	599	0.00	1.00	1.34	1.02
		GJ-B2-SH	N06° 32′ 56.08″, E100° 14′ 13.76″	Shale	0.18	0.01	0.00	0.01	590	0.00	1.00	1.22	1.11
		GJ-B3-SH	N06° 32′ 56.08″, E100° 14′ 13.76″	Shale	0.10	0.01	0.00	0.01	600	0.00	1.00	1.32	1.13

TOC, total organic carbon (wt%); S_1, volatile hydrocarbon (HC) content, mg HC/g rock; S_2, remaining HC generative potential, mg HC/g rock; T_{max}, temperature at maximum generation (°C); *PI*, production index = $S_1/(S_1+S_2)$; *HI*, hydrocarbon index = $S_2 \times 100$/TOC, mg HC/g rock; *PY*, petroleum yield = S_1+S_2; $\%VR_o$, vitrinite reflectance (%); $\%SBR_o$, solid bitumen reflectance (%)

Table 2 Biomarker ratios of the analysed seven representative shale samples illustrating source organic matter, depositional environment conditions and thermal maturity

Samples ID	Source of organic matter and depositional environment conditions												Thermal maturity ratios and parameters			
	Pr/Ph	Pr/C_{17}	Ph/C_{18}	CPI	C_{29}/C_{30}	G/C_{30}	HCR_{31}/HC_{30}	C_{27}/C_{29} regular steranes	Regular steranes (%)			Ts/Tm	C_{32} 22S/(22S + 22R)	C_{29} 22S/(22S + 22R)	C_{29} ββ/(ββ + αα)	M_{30}/C_{30}
									C_{27}	C_{28}	C_{29}					
GJ-A1-SH	0.71	0.21	0.15	0.94	0.72	0.11	0.24	0.61	27.9	26.5	45.6	1.36	0.54	0.35	0.77	0.09
GJ-A2-SH	1.00	0.27	0.17	1.00	0.72	0.06	0.35	0.84	36.4	20.1	43.5	1.38	0.56	0.29	0.63	0.10
GJ-A3-SH	1.25	0.28	0.20	0.94	0.73	0.08	0.25	0.62	26.3	31.2	42.4	1.40	0.62	0.50	0.65	0.08
GJ-A4-SH	1.25	0.30	0.17	1.02	0.58	0.11	0.25	0.75	30.6	28.6	40.8	1.70	0.60	0.48	0.76	0.08
GJ-A5-SH	1.67	0.20	0.14	0.95	0.73	0.10	0.34	0.67	15.4	27.3	57.3	1.30	0.62	0.40	0.77	0.12
GJ-A6-SH	1.50	0.33	0.16	1.02	0.66	0.11	0.27	0.66	29.1	26.6	44.3	1.60	0.57	0.44	0.73	0.06
GJ-A7-SH	0.93	0.52	0.27	1.16	0.85	0.04	0.30	0.88	31.7	32.6	35.8	2.25	0.68	0.50	0.72	0.08
GJ-A8-SH	1.36	0.23	0.19	0.94	0.81	0.07	0.26	0.72	26.9	28.6	44.5	1.41	0.60	0.43	0.69	0.08
GJ-A9-SH	1.11	0.28	0.20	1.01	0.76	0.06	0.25	0.70	18.4	30.3	51.3	1.58	0.64	0.47	0.70	0.10
GJ-A10-SH	1.25	0.33	0.16	1.12	0.80	0.10	0.28	0.84	31.4	25.8	42.8	1.53	0.57	0.38	0.72	0.09
GJ-A11-Sh	1.08	0.30	0.19	1.00	0.79	0.11	0.25	0.69	30.0	29.3	40.7	1.40	0.65	0.41	0.68	0.10
GJ-A12-SH	1.23	0.27	0.21	1.03	0.73	0.05	0.31	0.67	29.3	25.6	45.1	1.72	0.60	0.48	0.71	0.11

Pr, pristane; *Ph*, phytane; *CPI*, carbon preference index, $\{2(C_{23}+C_{25}+C_{27}+C_{29}) / (C_{22}+2[C_{24}+C_{26}+C_{28}]+C_{30})\}$; C_{29}/C_{30}, C_{29} norhopane/C_{30} hopane; G/HC_{30}, Gammacerane/C_{30} hopane; HCR_{31}/HC_{30}, C_{31} regular homohopane/C_{30} hopane; M_{30}/C_{30}, C_{30} moretane/C_{30} hopane; *Ts*, (C_{27} 18α (H)-22, 29, 30-trisnorneohopane); *Tm*, (C_{27} 17α (H)-22, 29, 30-trisnorhopane)

Table 3 Major (wt%) and trace element (ppm) compositions of the analysed Timah Tasoh Formation shale samples

Sample No	Sample ID	Formation/ group	Lithology	TS (wt%)	Major elements (wt%)										Trace elements (ppm)												
					SiO_2	Al_2O_3	TiO_2	Fe_2O_3	CaO	MgO	Na_2O	K_2O	K_2O/Al_2O_3	K_2O/Na_2O	V	Ni	Cr	Ga	Rb	Sr	Ba	U	Sr/Ba	V/Cr	V/Ni	Ga/Rb	V/(V + Ni)
1	GJ-A1-SH	Timah Tasoh	Shale	0.23	67.0	5.21	0.23	2.12	0.08	0.28	0.03	1.47	0.28	49.0	211.0	75.0	175.0	9.40	53.8	89.0	258.0	2.50	0.34	1.21	2.81	0.17	0.74
2	GJ-A2-SH	Timah Tasoh	Shale	0.21	72.0	5.38	0.28	2.21	0.13	0.33	0.08	1.52	0.28	19.0	193.0	75.0	120.0	8.70	52.7	83.0	251.0	2.70	0.33	1.61	2.57	0.16	0.72
3	GJ-A3-SH	Timah Tasoh	Shale	0.28	70.3	5.52	0.30	2.30	0.10	0.35	0.10	1.58	0.28	15.8	219.0	83.2	152.0	10.7	62.3	76.0	243.0	2.56	0.31	1.44	2.63	0.17	0.72
4	GJ-A4-SH	Timah Tasoh	Shale	0.34	68.6	6.34	0.26	2.28	0.15	0.29	0.06	1.62	0.26	24.2	206.0	79.5	149.0	9.89	70.3	92.0	278.0	2.75	0.33	1.38	2.60	0.14	0.72
5	GJ-A5-SH	Timah Tasoh	Shale	0.31	69.8	5.32	0.24	2.17	0.13	0.30	0.11	1.56	0.29	14.2	198.0	78.0	146.0	11.5	64.9	81.0	289.0	2.63	0.28	1.36	2.54	0.18	0.71
6	GJ-A6-SH	Timah Tasoh	Shale	0.28	67.3	5.82	0.25	2.28	0.09	0.28	0.10	1.61	0.30	16.1	210.0	80.1	153.0	10.3	55.6	77.0	250.0	2.63	0.33	1.37	2.62	0.18	0.72
7	GJ-A7-SH	Timah Tasoh	Shale	0.33	69.8	5.24	0.29	2.14	0.11	0.34	0.08	1.53	0.29	19.2	199.0	76.4	133.0	8.91	58.9	86.0	264.0	2.54	0.29	1.50	2.60	0.15	0.72
8	GJ-A8-SH	Timah Tasoh	Shale	0.29	71.3	6.01	0.24	2.24	0.13	0.29	0.05	1.49	0.25	29.8	195.0	77.9	146.0	9.53	64.1	89.0	271.0	2.72	0.30	1.34	2.50	0.15	0.71
9	GJ-A9-SH	Timah Tasoh	Shale	0.34	70.2	6.21	0.30	2.27	0.09	0.28	0.04	1.60	0.26	40.0	218.0	81.2	173.0	9.89	60.7	91.0	283.0	2.69	0.34	1.26	2.68	0.16	0.73
10	GJ-A10-SH	Timah Tasoh	Shale	0.25	69.3	5.92	0.27	2.18	0.14	0.34	0.09	1.50	0.25	16.7	201.0	79.9	125.0	8.90	59.4	86.0	255.0	2.52	0.33	1.61	2.52	0.15	0.72
11	GJ-A11-SH	Timah Tasoh	Shale	0.27	69.0	5.74	0.24	2.30	0.12	0.30	0.07	1.53	0.27	21.9	215.0	83.0	168.0	10.3	54.2	71.0	276.0	2.70	0.27	1.28	2.59	0.19	0.72
12	GJ-A12-SH	Timah Tasoh	Shale	0.24	70.3	6.19	0.28	2.16	0.09	0.31	0.08	1.49	0.24	18.6	194.0	76.7	148.0	11.0	67.9	90.0	283.0	2.74	0.29	1.31	2.53	0.16	0.72

TS, total sulphur\

Results and discussion

Petroleum source rock potential and organic matter richness

The richness of organic matter could be determined by calculating the amount of total organic carbon (TOC) conducted together with the analysis of bulk pyrolysis analysis (Behar et al. 2015). Total organic carbon higher than one (> 1 wt%) indicates a good source potential (Peters and Cassa 1994; Hunt 1996; Peters et al. 2005; McCarthy et al. 2011). The TOC content of the analysed shale samples varies from 0.10 to 5.28 wt%, suggesting poor to very good potential based on Peters and Cassa (1994) and McCarthy et al. (2011) classification. The hydrocarbon generative potential (S_2) measured through the Rock–Eval pyrolysis together with other related parameters is presented in Table 1.

The shale samples show low S_2 compared to S_1, ranging from 0 to 0.17 mg HC/g rock-based on Table 1, indicating that only three samples are considered to have a poor hydrocarbon-generating potential. However, other samples show fair to excellent hydrocarbon-generating potential, regarding the minimum TOC required for further analysis is 0.5 wt% (e.g. Bordenave 1993; Peters and Cassa 1994; Hunt 1996). Therefore, as Peters and Cassa (1994) defined, only twelve analysed samples reach the standard 0.5 wt% TOC and subsequently selected for further biomarker analysis.

Kerogen type and hydrocarbon generation potential

Understanding kerogen type (quality of organic matter) and quantity of organic matter from several bulk pyrolysis data studied. Such as the hydrogen index (HI, mg HC/g TOC) against T_{max} were used as performed by the earliest researchers (e.g. Peters and Cassa 1994; McCarthy et al. 2011; Hakimi et al. 2016; Ayinla et al. 2017). A cross-plot of HI vs T_{max} is commonly applied, as shown in Fig. 3. Based on Fig. 3, the Timah Tasoh Formation shale samples are mostly plotted in the stage of the post-mature zone of the dry gas generation window (type IV kerogen). As the results show lower HI and S_2 values (Table 1), the analysed Timah Tasoh Formation samples will not generate liquid hydrocarbons (Peters and Cassa 1994). As being dominated by type IV kerogen that composed of mostly inert constituents thus devoid of petroleum-generating potential, the capability to generate dry gaseous hydrocarbons could not be ruled out (Fuan 1991).

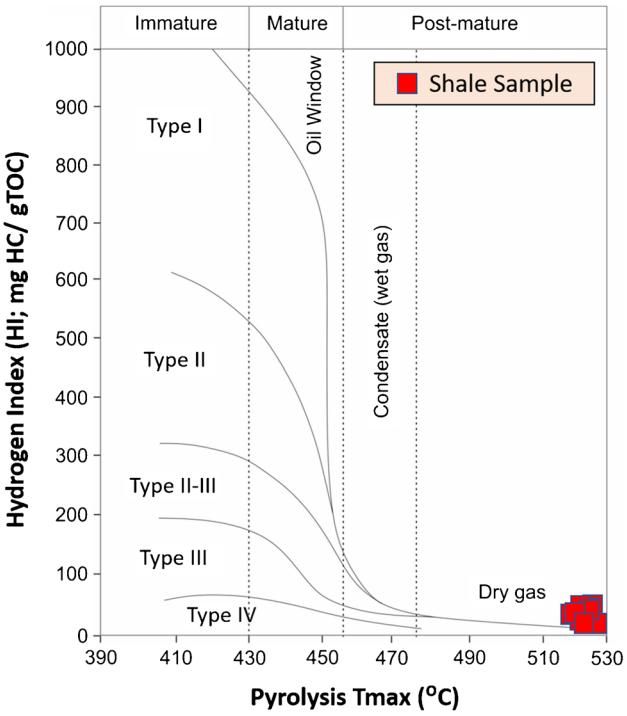

Fig. 3 Hydrogen index (HI, mg/TOC) versus maximum temperature at S_2 (T_{max}, °C) plot showing the high thermal maturity stage of the examined samples and characterised as type IV kerogen

Origin of organic matter and paleodepositional environment

n-Alkanes and isoprenoids

Biomarker fingerprint analysis of normal alkanes and isoprenoids is widely analysed, and selected measured ratios may interpret the origin of organic matter in both sediments and crude oil (Peters et al. 2005). Based on the bimodal fingerprints distribution in ion *m/z* 85 chromatogram (Fig. 4), a mixed source of organic matter input is the most probable interpretation for the analysed samples. Normal alkanes in these chromatograms are shown by the domination of medium to high molecular weight compounds of n-C_{15} to n-C_{33} and showing moderate height between odd and even n-alkanes. This n-alkane distribution supports the mixed source of organic matter input (Peters et al. 2005; Hakimi et al. 2020).

Acyclic isoprenoids especially pristane and phytane isoprenoids occur in a significant amount in the analysed samples. The pristane/phytane (Pr/Ph) ratios can provide an interpretation of the paleodepositional environment (Ten Haven et al. 1987; Peters and Moldowan 1993; Peters et al. 2005). Within the Timah Tasoh Formation shales, the value of Pr/Ph ranges from 0.71 to 1.67 (Table 2). These Pr/Ph values indicate that the analysed shales were deposited within

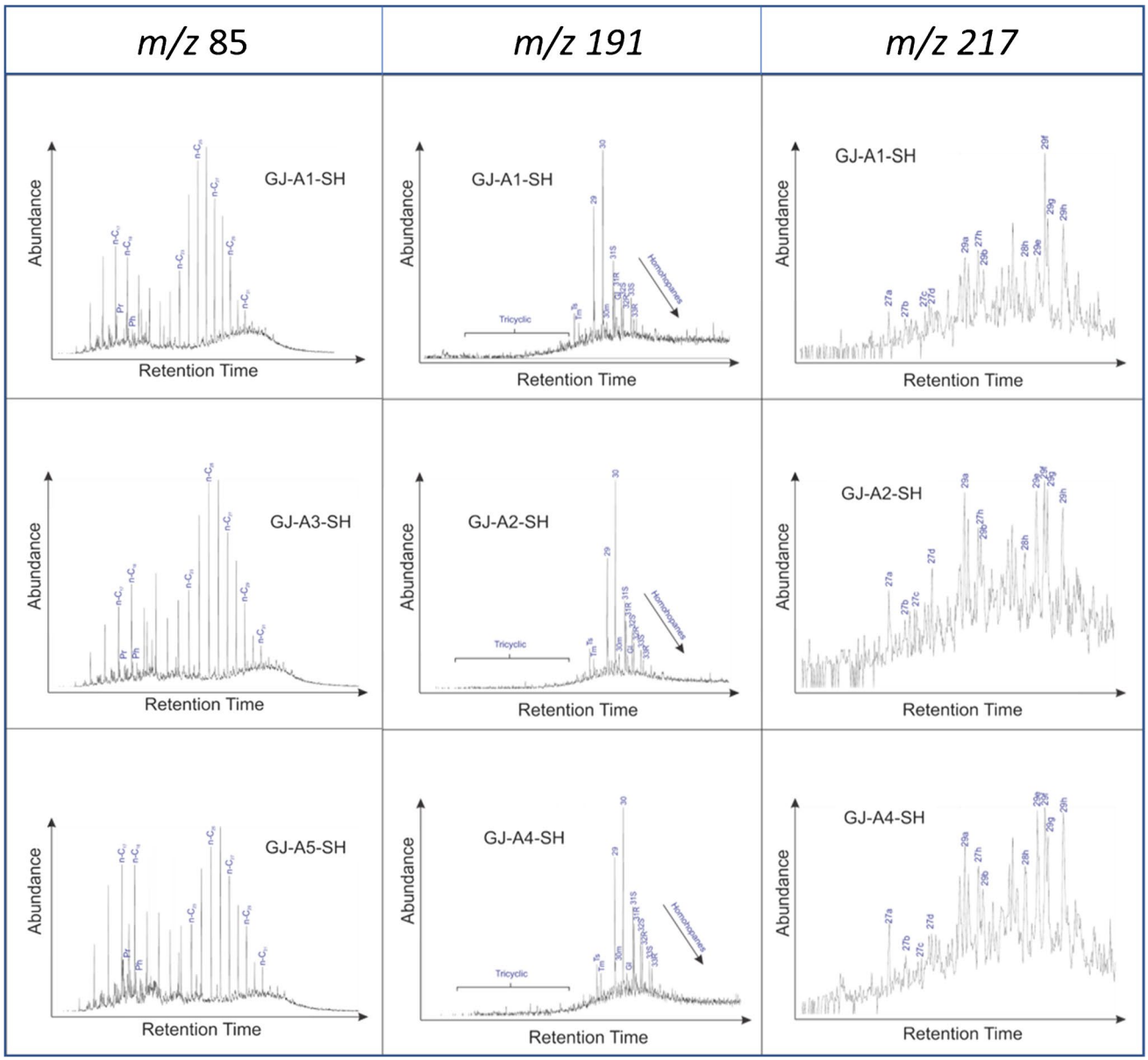

Fig. 4 The *m/z* 85, 191 and 217 mass fragmentograms of selected shale samples representing the distribution of *n*-alkanes, isoprenoids, triterpanes, terpanes, steranes and diasteranes

suboxic conditions of possibility in a mixed terrestrial-marine environment during the deposition of the sediments. These fingerprints have produced moderate values of carbon preference index (CPI) as presented in Table 2 ranging from 0.94 to 1.16. This CPI index is calculated to provide some insights into the source input of the organic matter (Peters et al. 2005). On the other hand, the low molecular weight compounds especially those below n-C_{23} are depleted, and this could be due to the weathering effects on the outcrop. However, the collected samples appear to be fresh in hand specimen. This is partly consistent with the low S_1 values determined from the Rock–Eval pyrolysis.

The results based on the Pr/Ph and CPI ratios can be corroborated by determining the correlation among the values of pristane/n-C_{17} and phytane/n-C_{18} ratios. Based on these ratios (Table 2), Pr/n-C_{17} and Ph/n-C_{18} ratios for the Timah Tasoh Formation range from 0.20 to 0.52 and 0.14 to 0.27 and have provided strong support for the origin of organic matter which is from a mixed organic matter source input. These sediments were most likely have been preserved under a suboxic condition within transitional environments deposited partially under reducing marine depositional environments (Fig. 5).

Hopanoid and steroid biomarker

The distribution of hopanoids and steroids among saturated hydrocarbon is commonly monitored on the fragmentograms of *m/z* 191 and 217 (Peters et al. 2005). According to Hunt (1996), hopanoids are important in petroleum hydrocarbon because they can maintain their habitual structure from the indigenous biological compounds. Ion *m/z* 191 of Timah Tasoh Formation is dominated by C_{27}, Ts, Tm, C_{29}, C_{30} hopane, and C_{30} to C_{34} homohopanes. The ion *m/z* 191 from the saturated hydrocarbon compounds shows many homohopanes than tricyclic terpanes, as shown in Fig. 4.

Peters et al. (2005) reported that the low abundance of tricyclic in these analysed samples suggests that these shale samples have considerable influence on terrestrial-derived organic matter, considering the high concentration of tricyclic terpanes is often associated with the marine environment. The homohopanes distributions from the analysed samples are controlled by the C_{31} homohopanes and decline to C_{34} homohopanes in a cascade pattern in the Timah Tasoh Formation (Fig. 4). According to Peters et al. (2005), Makeen et al. (2015) and Ayinla et al. (2017), the cascade pattern suggests that the organic matter was conserved in a suboxic condition. In the analysed ion *m/z* 191 fragmentograms, the C_{30} hopane in the Timah Tasoh Formation is more dominant than C29 hopane, which indicates the samples contain clay-rich sediments as reported from previous studies (e.g. Peters et al. 2005; Makeen et al. 2015).

In addition, the presence of gammacerane had initially been identified as an indicator of hypersalinity (Sinninghe Damsté et al. 1995; Makeen et al. 2015). Increasing salinity in both the marine and lacustrine environments has also been found to be associated with the presence of gammacerane (Waples and Machihara 1991; Peters and Moldowan 1993). In Table 2, the ratio of G/C_{30} from the analysed samples ranges from 0.04 to 0.11. The existence of gammacerane in the chromatograms of the Timah Tasoh Formation (Fig. 4) gives evidence of a slightly low salinity around the shale's deposition environments (e.g. Peters et al. 2005; Makeen et al. 2015).

The distribution of steroids is characterised from the *m/z* 217 fragmentograms. Steroids are another group of essential biomarkers that are derived from sterols found in higher plant and algae, but rare or absent in prokaryotic organisms (Seifert and Moldowan 1979). As an indication of variations in source environments, the comparable abundance of steranes C_{27}, C_{28}, and C_{29} in ion *m/z* 217 can be used for the study (Hunt 1996). The standard sterane abundance of C_{27}, C_{28}, and C_{29} is determined and calculated in Table 2. A ternary diagram modified from Huang and Meinschein (1979) is used to represent the results by plotting the steranes according to the regular members of the steranes, as shown in Fig. 6A. As the C_{29} is in the ranges of 35.8 to 57.3% relative to C_{27} and C_{28} (Table 2), the high percentage of C_{29} steranes confirms mixed organic source material interpretation. In the Timah Tasoh Formation sediments, these components of mixed organic matter were characterised by compositions of the source of planktonic, bacterial, and land-derived organic matter input. The result is consistent with the reduced C_{27}/C_{29} regular steranes deposition values in the suboxic condition (Fig. 6B), which was consistent with the decreasing hopane pattern in Fig. 4.

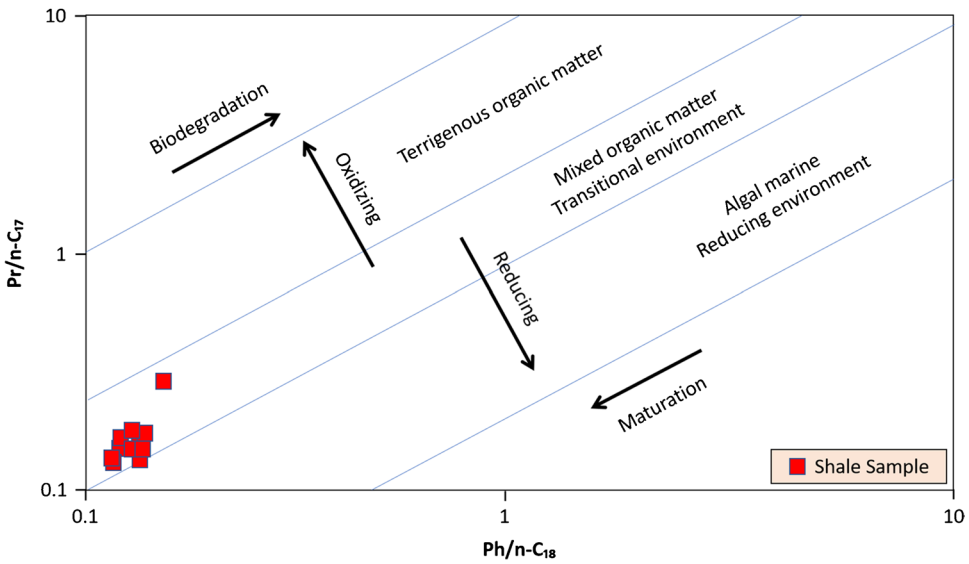

Fig. 5 Cross-plot of Pr/*n*-C_{17} versus Ph/*n*-C_{18} showing the organic matter input in the examined samples of the Timah Tasoh Formation

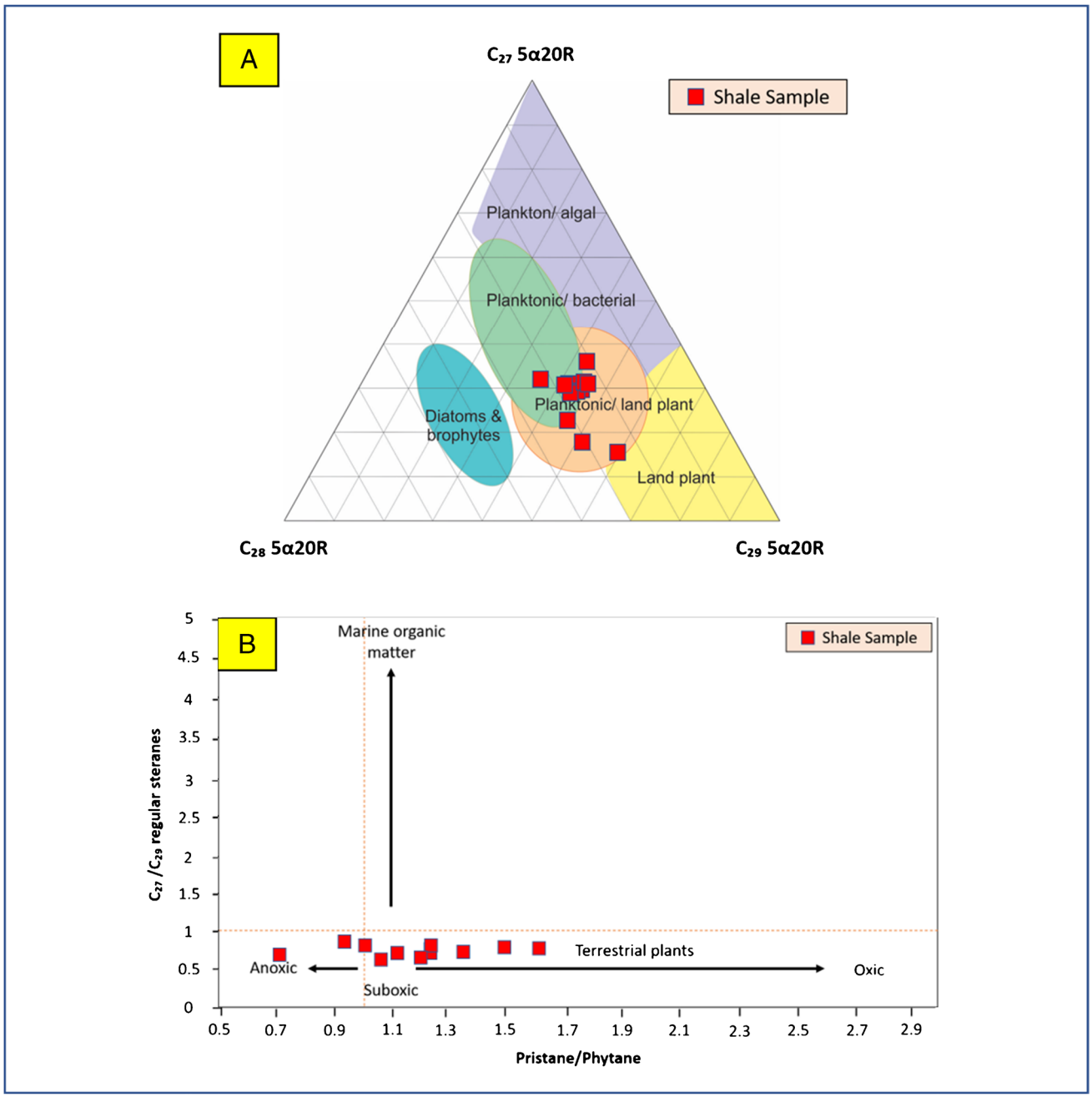

Fig. 6 (A) Ternary diagram of C_{27}, C_{28} and C_{29} regular steranes indicating a mixed organic matter input in the examined samples of the Timah Tasoh Formation. (B) Cross-plot of C_{31} 22R/C_{30} hopane versus Pristane/Phytane ratios of the examined samples (adapted after Peters et al. 2005)

Geochemistry of major and trace element

Paleoredox conditions during sedimentation

In addition to the GCMS biomarker identification, the geochemistry of the major oxides and trace elements measured from ICP-MS was also can be used to identify the paleodepositional condition and condition during sedimentation in the analysed sediments. From the concentration of trace elements, paleoredox conditions of sedimentary facies could be evaluated, primarily due to their strong association during the deposition in both sedimentary rocks and trace elements, as well as in the phases of kerogen transformation. Trace elements such as V, Ni, U, Th, Cr, Sr and Ba were used during sedimentation with specific standard ratios such as V/Ni and V/Cr applied to

determine redox conditions (Peters et al. 2005; MacDonald et al. 2010; Fu et al. 2011).

Vanadium (V) and nickel (Ni) are the significant metals usually present during the early diagenesis of organic matter and are valuable indicators of redox conditions of sedimentation (Peters et al. 2005; Galarraga et al. 2008). The reduced depositional environment can be interpreted by V/Ni > 3 and the suboxic environment (V/Ni from 1.9 to 3) based on the V/Ni ratio as described by Galarraga et al. (2008). Preferential vanadium enrichment over its paleoenvironmental marker (nickel) results in V/Ni ratios of the analysed range from 2.54 to 2.81 (Table 3). As seen in the vanadium (V) versus nickel (Ni) cross-plot in Fig. 7A, this result indicates the terrestrial source of organic matter preserved under suboxic to oxic conditions. Based on these values, throughout the organic matter sedimentation, the cross-relationship between low total sulphur content (ranging from 0.21 to 0.34) and moderate values of V/(V + Ni) ranging from 0.71

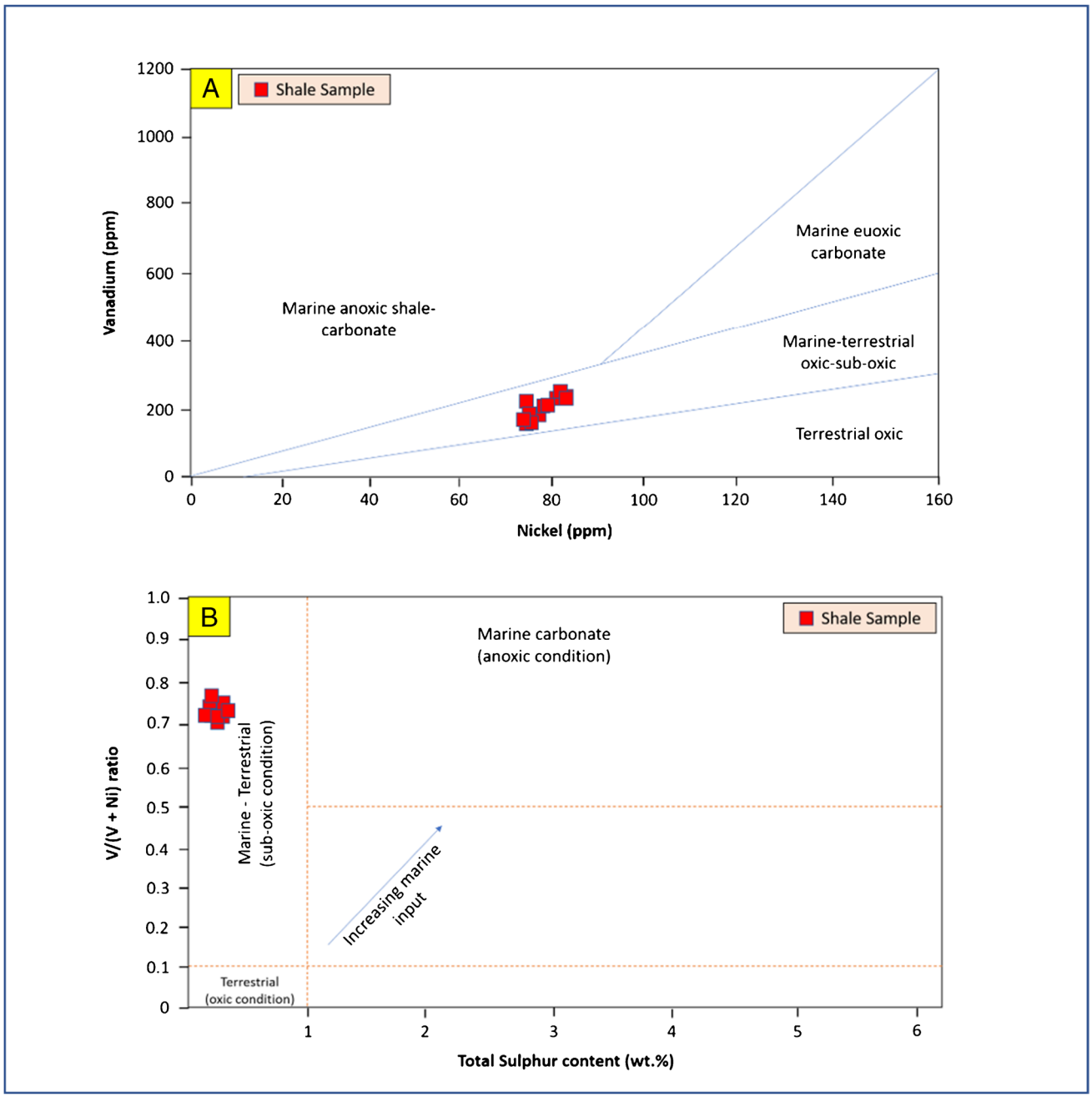

Fig. 7 Cross-plots of (A) vanadium (V) versus nickel (Ni) and (B) V/(V + Ni) versus total sulphur contents (TS, wt%) for paleodepositional environment conditions

to 0.74 generally confirms suboxic to oxic conditions of the analysed samples (Fig. 7B) (Barwise 1990).

In addition, the identification of chromium (Cr) and vanadium (V) concentration in the analysed samples can be used for the interpretation of paleoredox condition during sedimentation processes (Jones and Manning 1994). In oxic environments, the concentration of Cr is higher than in V and vice versa for anoxic conditions; therefore, Jones and Manning (1994) identified the V/Cr ratio above 2 as an anoxic environment indicator below 2 suggests suboxic to oxic conditions. A V/Cr ratio of between 1.21 and 1.61 ppm was seen in the studied samples (Table 3). This V/Cr ratio of the analysed samples further indicates the predominance of suboxic to oxic conditions during the organic matter sedimentation. Since various physical and chemical processes control organic matter preservation, other factors such as sedimentation rate, clay mineral content, and oxygenation levels of the water column are also reported to be involved in the sample preservation control (Zonneveld et al. 2010).

The concentrations of strontium (Sr) and barium (Ba) are crucial indicators of paleosalinity with a higher Sr/Ba ratio, perceived as high salinity, and low Sr/Ba ratio as a low salinity (Makeen et al. 2015, 2019). The analysed samples have a reasonably low Sr/Ba ratio (0.28 to 0.34 ppm), meaning that saline water has a relatively low effect during deposition, suggesting that the samples will be deposited in a stratified water column under suboxic conditions. Perhaps the low abundance of gammacerane lends (Fig. 4) supports this low salinity condition as the occurrence of gammacerane is often indicative of high salinity (as discussed in "Hopanoid and steroid biomarker" section).

Paleoclimatic conditions

For assessing paleoclimatic conditions in the samples studied, the composition, concentration and abundance of significant major oxides such as SiO_2, Al_2O_3, TiO_2 and K_2O are the important factors needed during the analysis (Suttner and Dutta 1986; Roy and Roser 2013; Makeen et al. 2019). Roy and Roser (2013) suggest that the amounts of SiO_2 and Al_2O_3 (Table 3) prove that the examined shale samples are derived from clay groups such as illite and kaolinite. The existence of aluminium (Al) and gallium (Ga) is usually enriched with kaolinite. It is correlated with the warm and humid climate. At the same time, illite is also correlated with potassium (K) and rubidium (Rb), indicating poor chemical weathering and dry and cold weather (Beckmann et al. 2005; Ratcliffe et al. 2004).

Many illite-rich sediments would have lower Ga/Rb and higher K_2O/Al_2O_3 ratios, while higher Ga/Rb and lower K_2O/Al_2O_3 ratios will have high kaolinite-rich deposits (Ratcliffe et al. 2004). The shales of the Timah Tasoh Formation have relatively low Ga/Rb ratios and high K_2O/Al_2O_3 ratios based on the results in Table 3. Indicating that illite clay mineral is higher than kaolinite clay mineral thus supports the interpretation of the predominance of illite mineral area (e.g. Baioumy et al. 2016). Therefore, Timah Tasoh Formation can be correlated to be formed during the arid climatic conditions. It is due to low water salinity during shale formation, as shown by low Sr/Br ratios (Table 3).

Organic matter optical characterisation and relation to thermal maturation

In this study, observed under the microscope, three types of macerals organic particles can be recognised under the microscope, which are recycled/reworked vitrinite, inertinite (Fig. 8A - D) and vitrinite-like bitumen or solid bitumen (Fig. 8E - H). Vitrinite-like bitumen or solid bitumen is a secondary organic matter substance mainly formed from converting the primary organic matter. Resulting from previous geological cycle exposure to relatively high temperatures (e.g. thermal alteration, burial tectonic pressure, and heating rate) that further caused the cracking of the primary organic matter (e.g. Jacob 1989; Jarvie et al. 2007; Mastalerz et al. 2018). In addition, the typical organic matter sequences of late to dry gas windows maturities are always significant to solid bitumen formation (Rippen et al. 2013; Hackley and Cardott 2016; Liu et al. 2019).

The optically observed bitumen was in the form of granular solid bitumen type in all of the analysed Timah Tasoh Formation samples which produced a dark grey in colour (Fig. 8E to H) with low reflections and displayed no fluorescence under blue light excitation. This solid bitumen was described either as fracture and void fillings or as dispersed particles inside the matrix of organic minerals (Landis and Castaño 1995). According to Cardott et al. (2015), as in the source rocks, the presence of solid bitumen suggests the existence of mature organic matter which can initially generate liquid hydrocarbons. The observation of the solid bitumen within samples indicates indigenous samples hosting post-oil solid bitumen, which originates and occurs in the exact location as the occurrence of trapped hydrocarbons suggesting that the examined solid bitumen is primarily a form of the residue of altered hydrocarbons. Post-oil solid bitumen could develop during thermal evolution as a primary solid bitumen or pre-existing hydrocarbons (Jarvie et al. 2007; Mastalerz et al. 2018). Therefore, it is likely an in situ solid primary oil migration remnant (Cardott et al. 2015).

The other organic components found in the analysed samples are reworked lighter grey vitrinite and macerals inertinite groups that give a slightly higher reflection than solid bitumen. Vitrinite reflectance measurement was carried out on the analysed samples of the Timah Tasoh Formation. The results are shown in Table 1. The formation

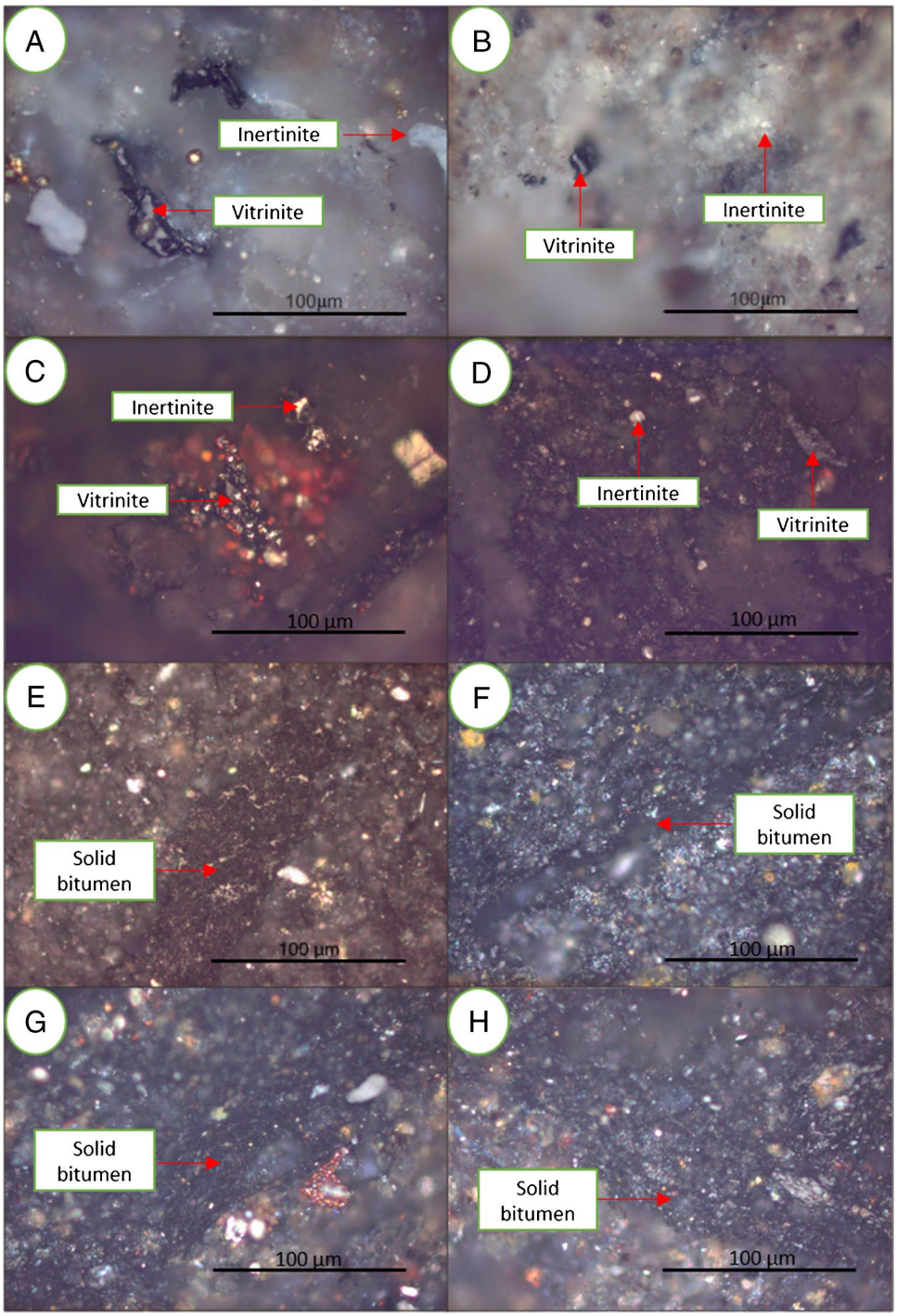

Fig. 8 Selected photomicrographs (A to H) of the analysed samples from the Timah Tasoh Formation. A to D Small fragments of highly reflecting inertinite phytoclasts suggesting recycled organic matter and light grey vitrinite particles. E to H Grey to dark-coloured angular solid bitumen accumulation in pore spaces and natural fractures

contains few primary vitrinite particles, and this has caused difficulties in taking the reflectance measurements. The photomicrographs of Fig. 8 show the common occurrence of a reworked organic matter, plenty of amorphous organic matter (AOM) and inertinite macerals of type IV kerogen. The Timah Tasoh Formation has vitrinite reflectance values with a range of 1.22 to 1.93%Ro. These ranges of values suggest a high thermal maturity for oil generation of late oil to dry gas window. Therefore, the analysed rocks can be classified as mature to overmature source rocks (e.g. Tissot and Welte 1984; Peters et al. 2005).

The occurrence of solid bitumen is pertinent when vitrinite is missing or absent and always related to high thermal maturity indicator (Landis and Castaño 1995). The relation of solid bitumen reflectance values and vitrinite reflectance values is commonly used among previous researchers in conducting thermal maturity evaluations (e.g. Bertrand 1993; Ferreiro Mählmann and Bayon 2016; Liu et al. 2017).

The reflectance values of solid bitumen vary from 1.05 to 1.39%SBRo (Table 1), which characterises the final stage of the oil window to the gas generation window. The results of vitrinite and solid bitumen reflectance reveal a clear linear association between these two organic matter components associated with an increase in the vitrinite reflectance maturity level and an increase in solid bitumen reflectance (e.g. Waliczek et al. 2019). Besides vitrinite reflectance, other various methods can be utilised for the interpretation of thermal maturity level in sedimentary rocks which includes pyrolysis (Espitalie et al. 1985), thermal alteration index (Staplin 1969) and conodont colour alteration index (Deaton et al. 1996). However, methods including vitrinite reflectance (%Ro), bulk pyrolysis (T_{max}, HI, PI, S_2) and interpretation of biomarker fingerprints remain the most common method used (Tissot and Welte 1984; Peters et al. 2005).

Based on the pyrolysis analysis, most of the analysed shale samples possess T_{max} values above 550 ºC (Table 1); this characteristic suggests that the organic matter has subjected to a high level of maturity. The gas generation window has been reached (Fig. 3), which is generally supported by the vitrinite reflectance and solid bitumen reflectance values discussed above. Apart from T_{max}, the production index (PI) ratio ($S_1/S_1 + S_2$) can be implemented to examine thermal maturity (Merril 1991). All of the analysed samples possess PI values > 0.25 (Table 1), thus in support of the high thermal maturity level (e.g. Merril 1991). The cross-plot between PI and T_{max} (Fig. 9A) shows that the analysed samples are in the gas generation window.

In addition, multiple biomarker parameters can also be used to assess the thermal maturity of the organic matter, such as the distribution of n-alkanes in the analysed samples, according to Waples and Machihara (1991) and Peters et al. (2005), as shown in *m/z* 85. The carbon preference index (CPI) ratio is commonly applied to determine maturity. CPI values below to one indicate as immature, while near to one indicates mature samples. Based on this study, the CPI ratios are in the range of 0.94 to 1.16 (Table 1) for the analysed samples, showing they are thermally matured. According to Peters et al. (2005) and Hakimi and Abdullah (2013), the C_{32} 22S/(22R + 22S) homohopanes ratio from *m/z* 191 is also commonly applied to assess thermal maturity. For the Timah Tasoh Formation, the C_{32} 22S/(22R + 22S) homohopanes range within 0.54 to 0.68 (Table 2) indicates the stage of oil generation already been outstretched or passed (Peters et al. 2005).

The moretane/hopane ratios concur with the organic matter being mature with values below 0.15 (e.g. Seifert and Moldowan 1979; Peters et al. 2005). According to Seifert and Moldowan (1986), the importance of moretane/hopane decreases with increasing thermal maturity. Moretane/hopane ratios of the Timah Tasoh samples range from 0.06 to 0.14 (Table 2). These calculated values reveal that the organic matter from the samples examined is at a high thermal maturity stage and thus supports the assessment based on the vitrinite reflectance measurements discussed earlier. In addition, according to Moldowan et al. (1986), although the ratio of Ts/Tm is known to be influenced by source facies, the Ts/Tm can be applied to measure and determine the thermal maturity level. As stated by Peters et al. (2005), during catagenesis, C_{27} 18 α-trisnohorpane (Ts) is more stable than C_{27} 17 α-trisnohorpane ratio (Tm). As can be observed in Fig. 4, Ts is more dominant compared to Tm, thus indicating that the analysed samples of the Timah Tasoh Formation are thermally matured. The cross-plot between C_{29} 22S/(22S + 22R) and ββ/(ββ + αα) sterane from the *m/z* 217 fingerprints is particularly constructive in explaining the thermal maturity of source rocks (Seifert and Moldowan 1986; Peters et al. 2005). The analysed samples of the Timah Tasoh Formation are mostly already passed the thermal equilibrium, thus consistent with their generation of post-mature source rocks (Seifert and Moldowan 1986) (Fig. 9b).

As noticed with the combination of organic geochemical and petrological results presented, most of the organic matter in the analysed shale samples from the Timah Tasoh Formation is shown to attain a significantly high thermal maturation stage by the measured vitrinite reflectance (%Ro). It can be applied to determine the paleoheat flow (Botor et al. 2019), which was influenced by the burial temperature and geological exposure period (Sweeney and Burnham 1990; Hakimi et al. 2020). These results can be explained or attributed to factors such as regional tectonic setting caused by collisional orogenesis and subduction of the Western Belt of Peninsular Malaysia that produced various tectonic deformation (Ghani et al. 2013; Metcalfe 2013b). And also, a consequence of thick overburden rocks of Late Devonian to Permian in Paleozoic age times (Hassan and Lee 2005). Then, the major of high heat flow from a mantle hotspot during the late Cretaceous times (Tjia 1998) caused a sudden high thermal temperature that has cooked all the sediments in the surrounding (Fig. 3).

Generation of thermogenic gas and the impacts on the future hydrocarbon exploration

Having the occurrence of solid bitumen as observed under the microscope suggests that the shale samples initially have the capability to produce liquid hydrocarbons (Cardott et al. 2015; Waliczek et al. 2019) which supported the generation potential being fair to excellent based on the initial TOC content before the overburden rocks caused the cracking of primary kerogen which altered its characteristics to type IV, thus resulted in the low HI values. Moreover, the high T_{max} indicates an increase in maturity (e.g. Peters et al. 2005; Dai et al. 2014). However, the high thermal temperature from the mantle hotspot caused the transformation of primary organic

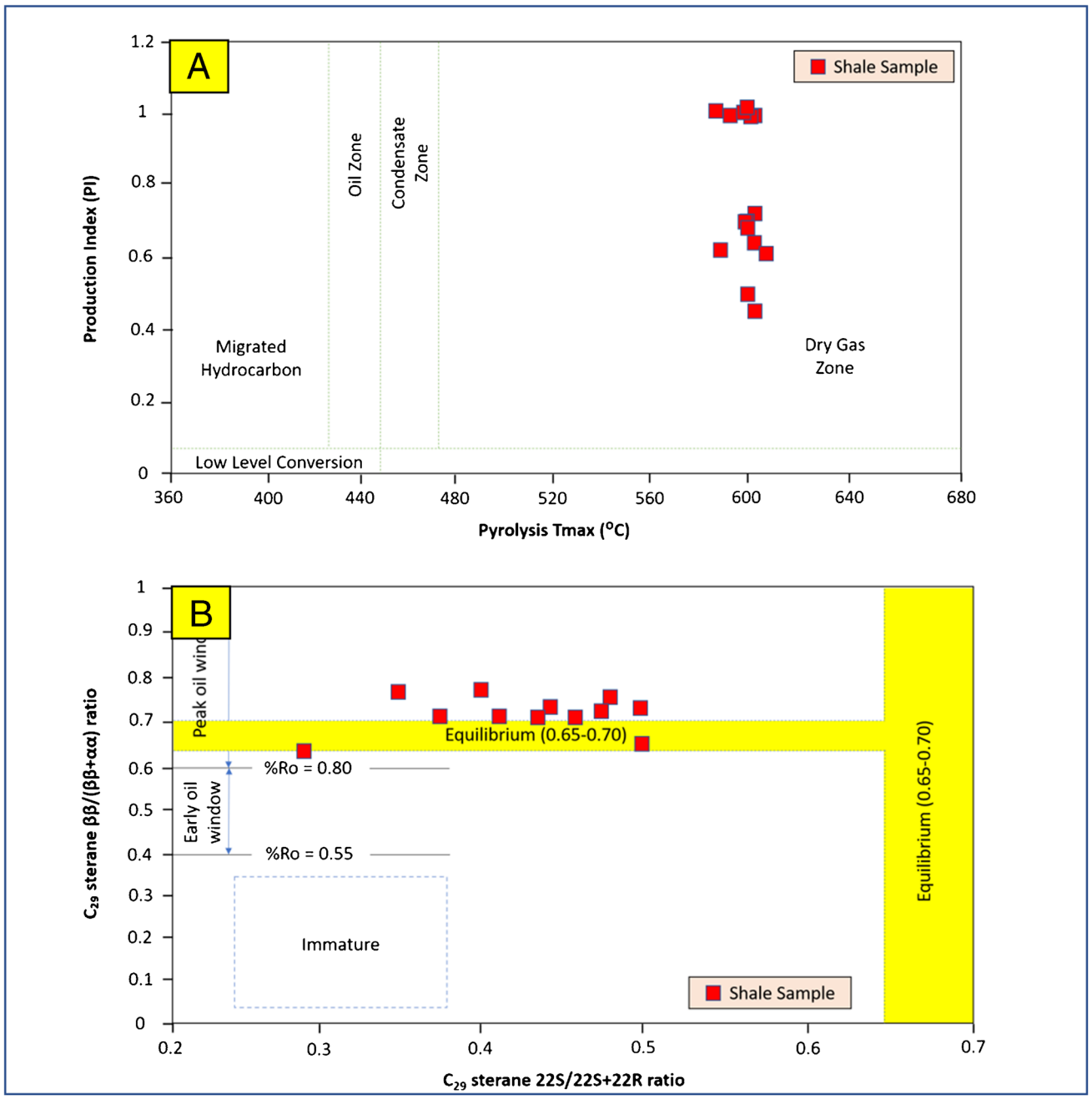

Fig. 9 (A) Pyrolysis T_{max} versus production index (PI), showing the maturation of the analysed shale samples. (B) The cross-plot of C_{29} sterane ββ/(ββ + αα) versus C_{29} sterane 22S/(22S + 22R) showing the thermal maturity level of the analysed Timah Tasoh Formation shales

matter to secondary organic matter (secondary cracking of bitumen) which consequently transformed the liquid/wet gaseous hydrocarbons into thermogenic gas.

In the analysed Timah Tasoh shales, the initial types of organic matter and their preservation during deposition were primarily demonstrated from the biomarker fingerprints of the residual organic matter. The lipid biomarkers in the saturated hydrocarbons suggest that mixtures of organic matter are from phytoplanktonic algae, bacterial and land plant inputs which present in the analysed Timah Tasoh shales. These phytoplankton/bacterial lipids and terrigenous organic matter indicate a mixture of predominantly types II and III kerogens as the original organic matter during deposition of the Timah Tasoh shales. The distributions of the biomarker in the examined shale samples indicate that the analysed samples were accumulated under substantial environmental conditions of water column reduction and stratification. These environmental conditions have thus

increased the preservation of organic matter and have consequently resulted in the organic matter being enriched during deposition.

However, these rich organic matter inputs derived from lipid biomarkers of the analysed Timah Tasoh shales are inconsistent with the geochemical pyrolysis results, in which the analysed samples consist mainly of type IV kerogen as indicated from their current low HI values. As shown by the high pyrolysis values (i.e. T_{max} and PI) and optical VR values of more than 1%, this probably is due to its high thermal maturation of the gas generation window, which may have depleted possible liquid hydrocarbons in which the high maturity is known to reduce the HI and TOC sample (Dai et al. 2014; Hakimi et al. 2020). Therefore, the shale intervals in the Devonian Timah Tasoh Formation of northern Peninsular Malaysia were, as a result of this, postulated to possess potential as a shale gas source rock (Fig 10).

It is most evident within the analysed Timah Tasoh samples in the study area. The significantly high thermal maturation experienced on the organic matter can be attributed to the high heat flow (> 110 mW/m^2) from a mantle hotspot during the end of Late Cretaceous times (Madon 1993; Tjia 1998), combined with the high overload rock thickness from late Triassic to late Cretaceous sequences. Consequently, in this analysis, the gas potential of the Timah Tasoh sediments is mainly thermogenic gas. It consists of two separate processes: the primary conversion of kerogen (types II and III) to oil and wet gas due to the high temperature of sedimentary rock thickness and the secondary cracking on the retention of generated oil and wet gas in the source rock system. This is regarded as the key to its inherent thermogenic gas potential.

Such a scenario of converting from the type II and III kerogen into type IV kerogen related to the high thermal maturation and reducing HI values from pyrolysis can also be found from other worldwide case studies. Hakimi et al. (2020) indicate that the Madbi Formation shales are a thermogenic gas potential in the Say'un-Masila Basin, Yemen. Most organic matter has TOC values of more than 1% and consists of large amounts of marine organic matter, influenced by the land plants environments. These Late Jurassic Madbi shales showing a good source rock, thus, indicate the Madbi Formation to have types II and III kerogen that initially could produce oil and gas.

The increase in burial temperature is due to overburden and the thickness of the sedimentary deposition that occurred from early Carboniferous to recent—leading to decreasing HI values of the organic matter—giving rise to high thermal maturity values (above 1.30%Ro) of this formation. Such high thermal maturity significantly changes the original organic matter (type II and III to type IV), which eventually caused the cracking of retained oil in the source rock. It conversely changes from oil into gas. It is the factor in the Say'un-Masila Basin generation of thermogenic gas.

Besides the high thermal maturity impact from the conditions of the tectonic event that generated thermogenic shale gas in the Timah Tasoh Formation, the conversions of this bitumen-to-gas generation can also be correlated with other potential petroleum sedimentary basin areas. Such as Katakolo Bay in Western Greece (e.g. Etiope et al. 2013) and Xiamaling Formation in the Xiahuayuan region (e.g. Xiong et al. 2016). Most of these thermogenic gas generation is mainly produced by secondary cracking of retained bitumen in highly mature and overmature shale. It is controlled by geological factors such as high thermal heat flow from the tectonic rifting events that caused various deformation events and controlled by the sediment burial history that influenced the increase of vitrinite reflectance values (Peters et al. 2005).

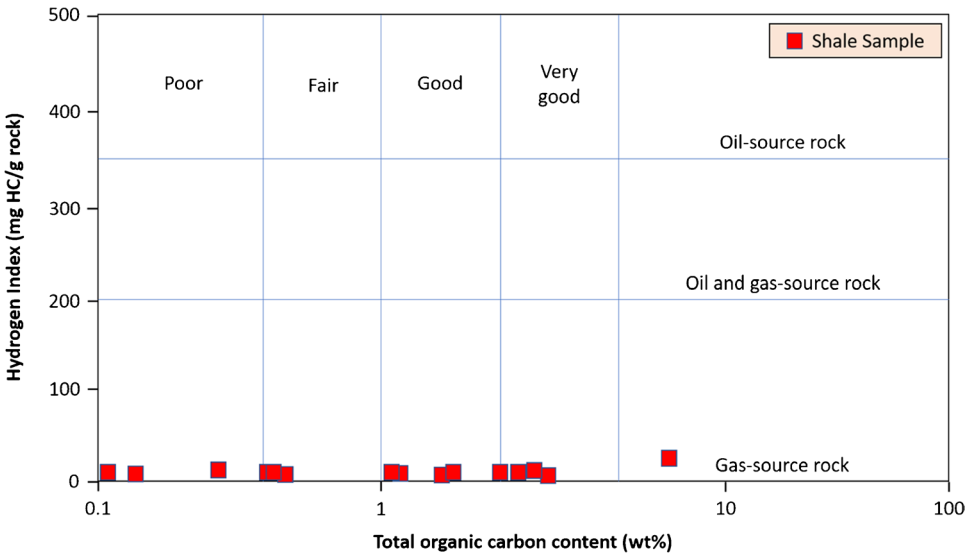

Fig. 10 Relationship between TOC content and HI values of the analysed shale samples in the Timah Tasoh Formation in northern peninsular Malaysia, showing gas generation potential

Therefore, the analysed Timah Tasoh Formation samples can generate thermogenic gas in the deeper parts of the Paleozoic succession. As the high maturity phase impacts the organic matter, which has already lost about 50% of its original organic carbon content (Hakimi et al. 2020), this could relate to the prospective hydrocarbon exploration in Malaysia and Southeast Asia.

Concluding remarks

At the end of the study, the integrated organic, inorganic geochemical and petrological study performed in this study on the Paleozoic shales of the Timah Tasoh Formation in northern Peninsular Malaysia has unravelled aspects of organic matter source input, paleodepositional environment, thermal maturity and the hydrocarbon generation potential. Therefore, the main research objectives which to understand the depositional condition setting of the source rock and also to determine the source rock potential for hydrocarbon generation can be fulfilled by the results as concluded as follows:

1. The analysed Timah Tasoh Formation shales possess TOC content ranging from 0.10 to 5.28 wt% and thus graded as poor to excellent source rocks.
2. The microscopical study showed that the shale samples are dominated by inertinite and recycled vitrinitic phytoclasts. The formation of solid bitumen supports the capability of the Timah Tasoh Formation shales to generate hydrocarbon.
3. Biomarker assemblages, petrographic, and pyrolysis data revealed that shales of the Timah Tasoh Formation contain primarily type IV kerogen of terrestrial-derived but showed the presence of marine influence. This mixed organic matter input suggests a transitional environment of deposition for the analysed sediments.
4. Based on the evaluation of the trace elements, the ratios of Sr, Ba, V, Ni and Cr indicated a stratified water column with low salinity and suboxic to oxic bottom water conditions.
5. Rock–Eval pyrolysis data, petrographic study and biomarker parameters of the analysed Timah Tasoh Formation shales show that the sediments are at a post-mature maturity level. However, they are presently most likely possessed gas potential for oil generation based on the high vitrinite reflectance and solid bitumen reflectance values.
6. This study, therefore, suggests that the shale sequences within the Paleozoic Timah Tasoh Formation have a variable potential of poor to excellent source rock with no remaining liquid hydrocarbon potential based on the very low HI values. And the organic matter is dominated by type IV kerogen, but they have thermogenic gas generation potential at deeper levels. The Timah Tasoh Formation itself can act as source rocks from the transformation of types II and III kerogens into type IV kerogen due to higher thermal maturation attributed to the high heat flow of a mantle hotspot during the later Late Cretaceous. Thus, the data produced can reference future petroleum exploration activities for conventional and unconventional hydrocarbon resources in this northern Peninsular Malaysia region.

Appendix

Table 4 The peak abbreviations from saturated fractions in the *m/z* 191 (I) and 217 (II)

(I) Peak No		
Ts	18α(H),22,29,30-trisnorneohopane	Ts
Tm	17α(H),22,29,30-trisnorhopane	Tm
29	17α,21β(H)-nor-hopane	C_{29} hop
30	17α,21β(H)-hopane	Hopane
30 M	17β,21α(H)-Moretane	C_{30}Mor
29 M	17β,21α(H)-30-norhopane	Normoretane
31S	17α,21β(H)-homohopane (22S)	C31(22S)
31R	17α,21β(H)-homohopane (22R)	C31(22R)
32S	17α,21β(H)-homohopane (22S)	C32(22S)
32R	17α,21β(H)-homohopane (22R)	C32(22R)
33S	17α,21β(H)-homohopane (22S)	C33(22S)
33R	17α,21β(H)-homohopane (22R)	C33(22R)
(II) Peak No		
a	13β,17α(H)-diasteranes 20S	Diasteranes
b	13β,17α(H)-diasteranes 20R	Diasteranes
c	13α,17β(H)-diasteranes 20S	Diasteranes
d	13α,17β(H)-diasteranes 20R	Diasteranes
e	5α,14α(H), 17α(H)-steranes 20S	ααα20S
f	5α,14β(H), 17β(H)-steranes 20R	αββ20R
g	5α,14β(H), 17β(H)-steranes 20S	αββ20S
h	5α,14α(H), 17α(H)-steranes 20R	ααα20R

Acknowledgements The authors take on the opportunity to acknowledge the management of the Department of Geology, the University of Malaya, for providing the facilities for the organic petrology and geochemistry analyses.

Funding The authors are also very grateful for the financial support provided by the Ministry of Higher Education, Malaysia, through research grant number FP045-2017A.

References

Ayinla HA, Abdullah WH, Makeen YM, Abubakar M, Jauro A, Yandoka BM, Abidin NS (2017) Source rock characteristics, depositional setting and hydrocarbon generation potential of Cretaceous coals and organic-rich mudstones from Gombe Formation, Gongola Sub-basin, Northern Benue Trough, NE Nigeria. Int J Coal Geol 173:212–226

Azman AG (2009) Plutonism. In: Hutchinson CS, Tan DNK (eds) Geology of Peninsular Malaysia. University of Malaya and Geological Society of Malaysia, Kuala Lumpur, pp 211–232

Baioumy H, Ulfa Y, Nawawi M, Padmanabhan E, Anuar MN (2016) Mineralogy and geochemistry of Palaeozoic black shales from Peninsular Malaysia: Implications for their origin and maturation. Int J Coal Geol 165:90–105

Barwise AJG (1990) Role of nickel and vanadium in petroleum classification. Energy Fuels 4:647–652

Basori MBI, Leman MS, Zaw K, Meffre S, Large RR, Mohamed KR, Zin MM (2018) Implications of U-Pb detrital zircon geochronology analysis for the depositional age, provenance, and tectonic setting of continental Mesozoic formations in the East Malaya Terrane. Peninsular Malaysia Geological Journal 53(6):2908–2917

Beckmann B, Flögel S, Hofmann P, Schulz M, Wagner T (2005) Orbital forcing of Cretaceous river discharge in tropical Africa and ocean response. Nature 437(7056):241–244

Behar F, Beaumont V, Penteado HLDB (2015) Rock-Eval 6 technology: performances and developments. Oil Gas Sci Technol 56:111–134

Bertrand R (1993) Standardization of solid bitumen reflectance to vitrinite in some Paleozoic sequences of Canada. Energy Sources 15:269–287

Bordenave ML (1993) Applied petroleum, geochemistry. Technip, Paris

Botor D, Golonka J, Zając J, Papiernik B, Guzy P (2019) Petroleum generation and expulsion in the Lower Palaeozoic petroleum source rocks at the SW margin of the East European Craton (Poland). Annales Societatis Geologorum Poloniae.

Boucot AJ, Johnson JG, Racheboeuf PR (1999) Early Devonian brachiopods from Saturn Province, southern Thailand. J Paleontol 73(5):850–859

Brett CE, Baird GC (1993) Taphonomic approaches to temporal resolution in stratigraphy. In Kidwell, S.M., and Behrensmeyer, A.K. (eds.), Taphonomic Approaches to Time Resolution in Fossil Assemblages. Paleontological Society Short Course 6, 250–274.

Burton C (1970) The palaeotectonic status of the Malay Peninsula. Palaeogeogr Palaeoclimatol Palaeoecol 7(1):51–60

Cardott BJ, Landis CR, Curtis ME (2015) Post-oil solid bitumen network in the Woodford Shale, USA — a potential primary migration pathway. Int J Coal Geol 139:106–113

Cocks L, Fortey R, Lee C (2005) A review of Lower and Middle Palaeozoic biostratigraphy in west peninsular Malaysia and southern Thailand in its context within the Sibumasu Terrane. J Asian Earth Sci 24(6):703–717

Dai J, Zou C, Liao S, Dong D, Ni Y, Huang J, Hu G (2014) Geochemistry of the extremely high thermal maturity Longmaxi shale gas, southern Sichuan Basin. Org Geochem 74:3–12

Dardour AM, Boote DRD, Baird AW (2004) Stratigraphic controls on Paleozoic petroleum systems, Ghadames Basin. Libya Journal of Petroleum Geology 27(2):141–162

Deaton JW, Branton SL, Simmons JD, Lott BD (1996) The effect of brooding temperature on broiler performance. Poult Sci 75(10):1217–1220

Espitalie J, Madec M, Tissot B, Mennig J, Leplat P (1977) Source rock characterization method for petroleum exploration. Offshore Technology Conference.

Espitalie J, Deroo G, Marquis F (1985) Rock-Eval pyrolysis and its application, Inst. Fr. Petrol, 72.

Etiope G, Christodoulou D, Kordella S, Marinaro G, Papatheodorou G (2013) Offshore and onshore seepage of thermogenic gas at Katakolo Bay (Western Greece). Chem Geol 339:115–126

Ferreiro Mählmann R, Bayon RL (2016) Vitrinite and vitrinite like solid bitumen reflectance in thermal maturity studies: Correlations from diagenesis to incipient metamorphism in different geodynamic settings. Int J Coal Geol 157:52–73

Foo KY (1983) The Paleozoic sedimentary rocks of Peninsular Malaysia-stratigraphy and correlation. Proceedings of the Workshop on Stratigraphic Correlation of Thailand and Malaysia 1:1–19

Fu X, Wang J, Zeng Y, Cheng J, Tano F (2011) Origin and mode of occurrence of trace elements in marine oil shale from the Shengli River Area, Northern Tibet. China Oil Shale 28(4):487–506

Fuan F (1991) Geochemical characteristics of type IV kerogen from lower paleozoic source rocks in the lower Yangtze area. J SE Asian Earth Sci 5(1–4):39–42

Galarraga F, Reategui K, Martïnez A, Martínez M, Llamas J, Márquez G (2008) V/Ni ratio as a parameter in palaeoenvironmental characterisation of nonmature medium-crude oils from several Latin American basins. J Petrol Sci Eng 61(1):9–14

Gasparrini M, Sassi W, Gale JF (2014) Natural sealed fractures in mudrocks: a case tudy tied to burial history from the Barnett Shale, Fort Worth Basin, Texas, USA. Mar Pet Geol 55:122–141

Ghani AA, Searle M, Robb L, Chung S (2013) Transitional I S type characteristic in the Main Range Granite, Peninsular Malaysia. J Asian Earth Sci 76:225–240

Hackley PC, Cardott BJ (2016) Application of organic petrography in North American shale petroleum systems: a review. Int J Coal Geol 163:8–51

Hakimi MH, Abdullah WH (2013) Organic geochemical characteristics and oil generating potential of the Upper Jurassic Safer shale sediments in the Marib-Shabowah Basin, western Yemen. Org Geochem 54:115–124

Hakimi MH, Abdullah WH, Shalaby MR (2011) Organic geochemical characteristics of crude oils from the Masila Basin, eastern Yemen. Org Geochem 42(5):465–476

Hakimi MH, Abdullah WH, Alqudah M, Makeen YM, Mustapha KA (2016) Organic geochemical and petrographic characteristics of the oil shales in the Lajjun area, Central Jordan: origin of organic matter input and preservation conditions. Fuel 181:34–45

Hakimi MH, Ahmed A, Mogren S, Shah SB, Kinawy MM, Lashin AA (2020) Thermogenic gas generation from organic-rich shales in the southeastern Say'un-Masila Basin, Yemen as demonstrated by geochemistry, organic petrology, and basin modelling. J Pet Sci Eng 192:107322

Hassan MH (2013) Facies Analysis of the Uppermost Kubang Pasu Formation, Perlis: a wave-and storm-influenced coastal depositional system. Sains Malaysiana 42:1091–1100

Hassan MH, Lee CP (2005) The Devonian-Lower Carboniferous succession in Northwest Peninsular Malaysia. J Asian Earth Sci 24(6):719–738

Hassan MH, Aung A, Becker R, Rahman NA, Ng TF, Ghani AA, Shuib MK (2014) Stratigraphy and palaeoenvironmental evolution of the mid-to-upper Palaeozoic succession in Northwest Peninsular Malaysia. J Asian Earth Sci 83:60–79

Hassan MH, Erdtmann BD, Wang-Xiaofeng, Peng LC (2013) Early Devonian graptolites and tentaculitids in northwest Peninsular Malaysia and a revision of the Devonian–Carboniferous stratigraphy of the region. Alcheringa: An Australasian Journal of Palaeontology, 37(1) 49-63

Huang W, Meinschein W (1979) Sterols as ecological indicators. Geochim Cosmochim Acta 43(5):739–745

Hughes WB, Holba AG, Dzou LIP (1995) The ratio of dibenzothiophene to phenanthrene and pristane to phytane as indicators of depositional environment and lithology of petroleum in source rocks. Geochim Cosmochim Acta 59:3581–3598

Hunt JM (1996) Petroleum geochemistry and geology, 2nd edn. Freeman, San Francisco, W. H., p 743

Jacob H (1989) Classification, structure, genesis and practical importance of natural solid oil bitumen ("migrabitumen"). Int J Coal Geol 11(1):65–79

Jarvie DM, Hill RJ, Ruble TE, Pollastro RM (2007) Unconventional shale-gas systems: the Mississippian Barnett Shale of north-central Texas as one model for thermogenic shale-gas assessment. AAPG Bull 91(4):475–499

Jones CR (1973) The Siluro-Devonian graptolite faunas of the Malay Peninsula. Overseas Geology and Mineral Resources 44:25

Jones CR (1981) The geology and mineral resources of Perlis, North Kedah and the Langkawi Island. Geological Survey Malaysia District Memoir 17:1–257

Jones B, Manning DA (1994) Comparison of geochemical indices used for the interpretation of palaeoredox conditions in ancient mudstones. Chem Geol 111(1–4):111–129

Khoo TT, Tan BK (1983) Geological evolution of Peninsular Malaysia. proceeding of workshop on stratigraphic correlation of Thailand and Malaysia, I: Technical papers, Geological Society of Malaysia, 253–290.

Landis CR, Castaño JR (1995) Maturation and bulk chemical properties of a suite of solid hydrocarbons. Org Geochem 22(1):137–149

Lee CP (2001) The occurrence of Scyphocrinites lobolith in the Upper Silurian Upper Setul limestone of Pulau Langgun, Langkawi, Kedah and Guar Senai, Berseri, Perlis. Annual Geological Conference, 2001.

Lee CP (2009) Paleozoic stratigraphy. In: Hutchinson CS, Tan DNK (eds) Geology of Peninsular Malaysia. University of Malaya and Geological Society of Malaysia, Kuala Lumpur, pp 55–86

Lee CP, Leman MS, Hassan K, Nasib BM, Karim R (2004) Stratigraphic lexicon of Malaysia. Geological Society of Malaysia, Kuala Lumpur, p 162

Lewan MD, Henry AA (2001) Gas: oil ratios for source rocks containing Type-I, -II, -IIS and -III kerogens as determined by hydrous pyrolysis. In: Dyman, T.S., Kuuskraa, V.A. (Eds.) Geologic Studies of Deep Natural Gas Resources. U.S. Geological Survey.

Liu B, Schieber J, Mastalerz M (2017) Combines SEM and reflected light petrography of organic matter in the New Albany shale: a prospective on organic porosity development with thermal maturation. Int J Coal Geol 184:57–72

Liu B, Schieber J, Mastalerz M (2019) Petrographic and micro-FTIR study of organic matter in the Upper Devonian New Albany shale during thermal maturation: implications for Kerogen transformation. Memoir 120: Mudstone Diagenesis: Research Perspectives for Shale Hydrocarbon Reservoirs, Seals, and Source Rocks, 165–188.

MacDonald R, Hardman D, Sprague R, Meridji Y, Mudjiono W, Galford J, Rourke M, Dix M, Kelto M (2010) Using elemental geochemistry to improve sandstone reservoir characterization: a case study from the Unayzah interval of Saudi Arabia. In: SPWLA 51st Annual Logging Symposium, 1–16.

Madon M (1993) Overview of the structural evolution of the Malay and Penyu basins. PETRONAS Research & Scientific Services, Project 123/92, Report No. RP5–93–02 (unpublished).

Maeyama D, Suzuki N, Kazukawa K, Ando H (2020) Residual gas in extensive stratified Miocene Izura carbonate concretions exhibiting thermogenic origin and isotopic fractionation associated with carbonate precipitation. Marine and Petroleum Geology, 119, 104466.

Makeen YM, Abdullah WH, Hakimi MH, Mustapha KA (2015) Source rock characteristics of the Lower Cretaceous Abu Gabra Formation in the Muglad Basin, Sudan, and its relevance to oil generation studies. Mar Pet Geol 59:505–516

Makeen YM, Abdullah WH, Ayinla HA, Shan X, Liang Y, Su S, Asiwaju L (2019) Organic geochemical characteristics and depositional setting of Paleogene oil shale, mudstone and sandstone from onshore Penyu Basin, Chenor, Pahang, Malaysia. Int J Coal Geol 207:52–72

Mastalerz M, Drobniak A, Stankiewicz AB (2018) Origin, properties, and implications of solid bitumen in source-rock reservoirs: a review. Int J Coal Geol 195:14–36

Maynard JB, Valloni R, Yu H (1982) Composition of modern deep-sea sands from arc-related basins. Geol Soc Lond Spec Publ 10(1):551–561

McCarthy K, Rojas K, Niemann M, Palmowski D, Peters K, Stankiewicz A (2011) Basic petroleum geochemistry for source rock evaluation. Oilf Rev 23:32–43

Merril RK (1991) Source and migration processes and evaluation techniques (R.K., Merril, ed.), American Association of Petroleum Geologists, Tulsa, Oklahoma.

Metcalfe I (1988) Origin and assembly of southeast Asian continental terranes. In Audley-Charles MG, Hallam A (eds) Gondwana and tethys. Geological Society of London Special Publication, 37, pp 101–118

Metcalfe I (2013) Gondwana dispersion and Asian accretion: tectonic and palaeogeographic evolution of eastern Tethys. J Asian Earth Sci 66:1–33

Metcalfe I (2013) Tectonic evolution of the Malay peninsula. J Asian Earth Sci 76:195–213

Metcalfe I (2017) Tectonic evolution of Sundaland. Bull Geol Soc Malaysia 63:27–60

Moldowan JM, Sundararaman P, Schoell M (1986) Sensitivity of biomarker properties to depositional environment and/ or source input in the Lower Toarcian of S.W.Germany. Org Geochem 10:915–926

Newport Leo P, Aplin AC, Gluyas JG, Chris Greenwell H, Gröcke DR (2016) Geochemical and lithological controls on a potential shale reservoir: Carboniferous Holywell Shale, Wales. Mar Pet Geol 71:198–210

Nugraheni R, Sum C, Rahman AA (2013) A review of shale gas prospects from non-marine shales in Indonesia and Malaysia - a new beginner in shale gas play. London 2013, 75th Eage Conference En Exhibition Incorporating SPE Europec.

Peters KE, Moldowan JM (1993) The biomarker guide: interpreting molecular fossils in petroleum and ancient sediments. Prentice-Hall Inc, Eaglewood Cliffs, New Jersey

Peters KE, Clark ME, das Gupta U, McCaffrey MA, Lee CY (1995) Recognition of an Infracambrian source based on biomarkers in the Bagehwala-1 oil, India. AAPG Bull 79:1481–1494

Peters KE, Walters CC, Moldowan JM (2005) The biomarker guide, 2nd edn. Cambridge University Press, Cambridge, UK

Peters KE, Cassa MR (1994) Applied source rock geochemistry. In: Magoon, I.B., Dow, W.G., (Eds.), The petroleum system-from source to trap. American Association of Petroleum Geologist Memoir, 60, 93–120.

Pytlak L, Gross D, Sachsenhofer R, Bechtel A, Gratzer R, Linzer H (2016) Generation, mixing and alteration of thermogenic and microbial gas in oil deposits: the case of the Alpine Foreland Basin (Austria). Mar Pet Geol 78:575–592

Radke M (1987) Organic geochemistry of aromatic hydrocarbons. In: Brooks J, Welde D (eds) Advances in Petroleum Geochemistry, vol 2. Academic Press, London, pp 141–205

Radke M, Welte DH, Willsch H (1986) Maturity parameters based on aromatic hydrocarbons: influence of the organic matter type. Org Geochem 10:51–63

Ratcliffe KT, Wright AM, Hallsworth C, Morton A, Zaitlin BA, Potocki D, Wray DS (2004) An example of alternative correlation techniques in a low-accommodation setting, nonmarine hydrocarbon system: the (Lower Cretaceous) Mannville Basal Quartz succession of southern Alberta. AAPG Bull 88(10):1419–1432

Rippen D, Littke R, Bruns B, Mahlstedt N (2013) Organic geochemistry and petrography of Lower Cretaceous Wealden black shales of the Lower Saxony Basin: the transition from lacustrine oil shales to gas shales. Org Geochem 63:18–36

Rooney MA, Claypool GE, Chung HM (1995) Modelling thermogenic gas generation using carbon isotope ratios of natural gas hydrocarbons. Chem Geol 126(3–4):219–232

Roser BP, Korsch RJ (1986) Determination of tectonic setting of sandstone-mudstone suites using SiO_2 content and K_2O/Na_2O ratio. J Geol 94(5):635–650

Ross DJK, Bustin RM (2009) The importance of shale composition and pore structure upon gas storage potential of shale gas reservoirs. Mar Pet Geol 26:916–927

Roy DK, Roser BP (2013) Climatic control on the composition of Carboniferous Permian Gondwana sediments, Khalaspir basin. Bangladesh Gondwana Research 23(3):1163–1171

Scrivenor JB (1928) The geology of Malaysian ore deposits. MacMillan Press, London, p 216

Scrotchman IC (2016) Shale gas and fracking: exploration for unconventional hydrocarbons. Proc Geol Assoc 127:535–551

Seifert WK, Moldowan JM (1979) The effect of biodegradation on steranes and terpanes in crude oils. Geochim Cosmochim Acta 43(1):111–126

Seifert WK, Moldowan JM (1986) Use of biological markers in petroleum exploration. In: Johns RB (ed) Methods in Geochemistry and Geophysics, vol 24. Elsevier, Amsterdam, pp 261–290

Sinninghe Damsté JS, Kenig F, Koopmans MP, Köster J, Schouten S, Hayes JM, de Leeuw JW (1995) Evidence for Gammacerane as an indicator of water column stratification. Geochimica Et Cosmochimica Acta 59(9):1895–1900

Soua M (2014) Paleozoic oil/gas shale reservoirs in southern Tunisia: an overview. J Afr Earth Sc 100:450–492

Staplin FL (1969) Sedimentary organic matter, organic metamorphism, and oil and gas occurrence. Bull Can Pet Geol 17(1):47–66

Staufer PH, Mantajit N (1981) Late paleozoic tilloids of Malaya, Thailand and Burma. In: Hambrey MJ, Halland WB (eds) Earth's pre-Pleistocene glacial record. Cambridge University Press, pp 331–337

Suttner LJ, Dutta PK (1986) Alluvial sandstone composition and paleoclimate. 1. Framework mineralogy. SEPM Journal of Sedimentary Research 56:329–345

Sweeney JJ, Burnham AK (1990) Evaluation of a simple model of vitrinite reflectance based on chemical kinetics. AAPG Bull 74:1559–1570

Ten Haven HL, de Leeuw JW, Rullkotter J, Sinnighe Damste JS (1987) Restricted utility of the pristane/phytane ratio as a paleoenvironmental indicator. Nature 330:641–643

Tissot BP, Welte DH (1984) Petroleum formation and occurrence, 2nd edn. Springer, New York

Tjia HD (1998) Origin and tectonic development of Malay-Penyu-West Natuna basins. Bull Geol Soc Malaysia 42:147–160

Tourtelot Harry A (1979) Black shale - its deposition and diagenesis 1. Clays Clay Miner 27(5):313–321

Tunstall T (2015) Iterative bass model forecasts for unconventional oil production in the Eagle Ford Shale. Energy 93:580–588

Vanhazebroeck E, Borrok DM (2016) A new method for the inorganic geochemical evaluation of unconventional resources: an example from the Eagle Ford Shale. J Nat Gas Sci Eng 33:1233–1243

Waliczek M, Machowski G, Więcław D, Konon A, Wandycz P (2019) Properties of solid bitumen and other organic matter from Oligocene shales of the Fore-Magura Unit in Polish Outer Carpathians: microscopic and geochemical approach. Int J Coal Geol 210:103206

Waples DW, Machihara T (1991) Biomarkers for geologist-a practical guide to the application of steranes and triterpanes in petroleum geology. Association of Petroleum Geologist. Methods in Exploration No.9, 91.

Welte D, Yalçin M (1988) Basin modelling—a new comprehensive method in petroleum geology. Organic Geochemistry In Petroleum Exploration, 141–151.

Xiong Y, Zhang L, Chen Y, Wang X, Li Y, Wei M, Lei R (2016) The origin and evolution of thermogenic gases in organic-rich marine shales. J Petrol Sci Eng 143:8–13

Zonneveld KA, Versteegh GJ, Kasten S, Eglinton TI, Emeis K, Huguet C, Wakeham SG (2010) Selective preservation of organic matter in marine environments; processes and impact on the sedimentary record. Biogeosciences 7(2):483–511

Zou C, Yang Z, Zhang G, Hou L, Zhu R, Tao S, Wu N (2014) Conventional and unconventional petroleum "orderly accumulation": concept and practical significance. Pet Explor Dev 41(1):14–30

Zou C, Yang Z, Dai J, Dong D, Zhang B, Wang Y, Pan S (2015) The characteristics and significance of conventional and unconventional Sinian-Silurian gas systems in the Sichuan Basin, central China. Mar Pet Geol 64:386–402

Zou C, Zhu R, Chen ZQ, Ogg JG, Wu S, Dong D, Zhen Q, Wang Y, Wang L, Lin S, Cui J, Su L, Yang Z (2019) Organic-matter-rich shales of China. Earth Sci Rev 189:51–78

Zumberge J, Ferworn K, Brown S (2012) Isotopic reversal ('rollover') in shale gases produced from the Mississippian Barnett and Fayetteville formations. Mar Pet Geol 31(1):43–52